



UNIVERSIDADE ESTADUAL DE CAMPINAS
FACULDADE DE ENGENHARIA DE ALIMENTOS

BRUNA CRISTINA GALLO

**ESTIMATE OF SOIL EROSION IN SUGARCANE AREAS BASED
ON GEOPROCESSING TOOLS**

**ESTIMATIVA DA EROSÃO DE SOLO EM ÁREAS DE CANA-DE-
AÇUCAR BASEADA EM FERRAMENTAS DE GEOTECNOLOGIA**

CAMPINAS

2023

BRUNA CRISTINA GALLO

**ESTIMATE OF SOIL EROSION IN SUGARCANE AREAS BASED
ON GEOPROCESSING TOOLS**

**ESTIMATIVA DA EROSÃO DE SOLO EM ÁREAS DE CANA-DE-
AÇUCAR BASEADA EM FERRAMENTAS DE GEOTECNOLOGIA**

Thesis presented to the Faculty of Food Engineering of the University of Campinas in partial fulfillment of the requirements for the degree of Doctor in Sciences.

Tese apresentada à Faculdade de Engenharia de Alimentos da Universidade Estadual de Campinas como parte dos requisitos exigidos para obtenção do título de Doutora em Ciências.

Supervisor/Orientador: Prof. Dr. Paulo Sérgio Graziano Magalhães

Este exemplar corresponde a versão final da tese defendida pela aluna Bruna Cristina Gallo, e orientada pelo Prof. Dr. Paulo Sérgio Graziano Magalhães.

CAMPINAS

2023

Ficha catalográfica
Universidade Estadual de Campinas
Biblioteca da Faculdade de Engenharia de Alimentos
Claudia Aparecida Romano - CRB 8/5816

G137e Gallo, Bruna Cristina, 1984-
Estimate of soil erosion in sugarcane areas based on geoprocessing tools /
Bruna Cristina Gallo. – Campinas, SP : [s.n.], 2023.

Orientador: Paulo Sergio Graziano Magalhães.
Tese (doutorado) – Universidade Estadual de Campinas, Faculdade de
Engenharia de Alimentos.

1. Degradação do solo. 2. Sensoriamento remoto. 3. Resíduos agrícolas. 4.
Palha. 5. Cana-de-açúcar. 6. Bioenergia. I. Magalhães, Paulo Sergio Graziano.
II. Universidade Estadual de Campinas. Faculdade de Engenharia de
Alimentos. III. Título.

Informações Complementares

Título em outro idioma: Estimativa da erosão de solo em áreas de cana-de-açúcar baseada em ferramentas de geotecnologia

Palavras-chave em inglês:

Soil degradation

Remote sensing

Crop residue

Straw

Sugarcane

Bioenergy

Área de concentração: Bioenergia

Titulação: Doutora em Ciências

Banca examinadora:

Paulo Sergio Graziano Magalhães [Orientador]

Rubens Augusto Camargo Lamparelli

Isabella Clerici de Maria

Tiago Osório Ferreira

Maurício Roberto Cherubin

Data de defesa: 29-06-2023

Programa de Pós-Graduação: Bioenergia

Identificação e informações acadêmicas do(a) aluno(a)

- ORCID do autor: <https://orcid.org/0000-0003-2556-4243>

- Currículo Lattes do autor: <https://lattes.cnpq.br/5650464536525125>

FOLHA DE APROVAÇÃO DA BANCA EXAMINADORA

Prof. Dr. Paulo Sérgio Graziano Magalhães – Presidente
NIPE/UNICAMP

Prof. Dr. Rubens Augusto Camargo Lamparelli – Membro Titular
NIPE/UNICAMP

Profa. Dra. Isabella Clerici de Maria – Membro Titular
IAC

Prof. Dr. Tiago Osório Ferreira – Membro Titular
ESALQ/USP

Prof. Dr. Mauricio Roberto Cherubin – Membro Titular
ESALQ/USP

A ata da defesa com as respectivas assinaturas dos membros encontra-se no SIGA/Sistema de Fluxo de Dissertação/Tese e na Secretaria do Programa da Unidade

Aos meus pais Rosangela Splendore Gallo e Carlos Antônio Gallo e avos Hermelinda Baseio Splendore (*in memoriam*), Otavio Splendore (*in memoriam*), Claudete Spagliario e Gilberto João Gallo (*in memoriam*), que nunca mediram esforços para minha educação.

À minha filha Ísis Gallo Sato, meu marido Marcus Vinicius Sato, meu irmão Carlos Antonio Gallo Junior, minha irmã Viviane Gallo Bertolla e sobrinhas Júlia Gallo Bertolla e Livía Gallo Bertolla pela força, cumplicidade e incentivo em todos os momentos da minha vida.

Com imenso carinho,

Dedico

À Sociedade Brasileira,

Ofereço

AGRADECIMENTOS

Ao criador de tudo que existe pela vida, oportunidades e pessoas que colocou em meu caminho.

Ao pesquisador e professor Dr. Paulo Sérgio Graziano Magalhães pela orientação, incentivo, reflexões e confiança na condução desse trabalho. Agradeço por todo conhecimento compartilhado ao longo desses anos.

Ao pesquisador Dr. João L. N. Carvalho e José Alexandre Melo Demattê, agradeço por todo apoio como co-orientador, pelos ensinamentos e disposição em sempre me ajudar nesse período de doutorado.

À Universidade Estadual de Campinas (UNICAMP) e ao Programa Integrado de Pós-Graduação em Bioenergia, pelo ensino de qualidade do curso de Doutorado. Ao Laboratório Nacional de Biorrenováveis (LNBR) e ao Centro Brasileiro de Pesquisa em Energia e Materiais (CNPEM), pelas facilidades oferecidas, pela oportunidade de realizar meu projeto de doutorado e aprender com pessoas excepcionais.

Agradeço pela concessão das bolsas de doutorado e apoio da Coordenação de Aperfeiçoamento de Pessoal de Nível Superior (CAPES) – Código de Financiamento 001.

Ao Projeto Sugarcane Renewable Electricity - SUCRE/PNUD (grant number BRA/101G31), e Fundação de Amparo à Pesquisa do Estado de São Paulo - FAPESP (# 2014/22262-0, # 2014/14965-0, # 2015/01587-0, and # 2017/03207-6) pelo auxílio financeiro para esse estudo.

À Prof. Dra. Dongmei Chen pela orientação durante o desenvolvimento dessa Tese na Queen's University e pela bolsa oferecida pelo Emergem Leaders in the American Program (ELAP) da Global Affairs Canada.

Ao GeoCis (<http://esalqgeocis.wixsite.com/english>), agradeço pelas discussões e sugestões no desenvolvimento desse trabalho.

À banca examinadora do doutorado, pelas reflexões e cordialidade em suas contribuições que foram fundamentais para meu crescimento pessoal e aos membros da primeira e segunda qualificação do doutorado, pelas excelentes contribuições para os capítulos desta tese: Dr. Rubens A. C. Lambarelli, Dr. Carlos E. P. Cerri, Dra. Isabella Clerici De Maria, Dr. Maurício R. Cherubin, Dr. Benito R. Bonfatti, Profa. Dong Mei e Tiago Osório Ferreira.

Aos pesquisadores Ricardo Bordonal e Walter Cervi, pelas valiosas contribuições, conhecimentos compartilhados para o desenvolvimento da metodologia desta tese.

À toda minha família, pela amizade, amor e incentivo nessa caminhada, a quem dedico essa tese. Ao meu companheiro Marcus Vinicius Sato, pelo constante incentivo, apoio,

paciência, amizade, risadas e amor durante todos esses anos e agradeço especialmente minha filha Isis, por me ajudar a viver o presente momento.

Aos queridos amigos, Leandro Barbosa, Sara Tenelli, Carla S'antana, Djanira, Camila Netto, Leandro Carolino, Guilherme Castioni, João Neto Bernardo Borges e Sérgio Castro pela amizade, momentos especiais compartilhados e por contribuírem, cada um à sua maneira, para minha formação intelectual.

Às amigas Sylvie, Donna, Beth, Suzane, Jenica, Jen, Hanna, Suzana, Martha e todas as outras colegas que fiz em Kingston/Ontario pela hospitalidade, atenção, amizade e momentos felizes durante o sanduiche no Canadá.

Aos professores do Programa de Estágio Docente (PED), a Profa. Priscilla Efraim e o Prof. Jansle V. Rocha, por me ajudarem a ampliar a visão acadêmica.

À usina Zilor pelo fornecimento dos locais experimentais e da assistência na instalação e condução dos experimentos e coleta de solos.

E à todos aqueles que, embora não citados nesse texto, tiveram uma contribuição importante durante essa etapa da minha carreira!

Muito obrigada!

RESUMO

A expansão intensiva de terras agrícolas para uma população crescente tem impulsionado a degradação do solo em todo o mundo. A modelagem de como os agroecossistemas respondem às variações nos atributos do solo, relevo e dinâmica do manejo da cultura pode orientar a conservação do solo. Esta pesquisa apresenta uma nova abordagem para avaliar a perda de solo por erosão hídrica em áreas cultivadas usando o modelo RUSLE e séries temporais de variáveis ambientais, agrícolas e antrópicas de sensoriamento remoto na região Sudeste do Estado de São Paulo, Brasil. A disponibilidade das imagens de satélite de acesso aberto da Tropical Rainfall Measuring Mission (TRMM) e imagens de satélite Landsat forneceram dez anos de dados de precipitação e 35 anos de superfície de solo exposto. A superfície nua do solo e o uso agrícola da terra foram extraídos e a erosividade pluviométrica multitemporal foi avaliada. Preveamos os atributos dos mapas de solo (textura e matéria orgânica) por meio de técnicas inovadoras de espectroscopia de solo para avaliar a erodibilidade do solo e a tolerância à perda de solo. A erosividade, erodibilidade e topografia obtidas por imagens de observação da Terra foram adquiridas para estimar a erosão do solo em quatro cenários de cobertura de palha da cana-de-açúcar (*Saccharum spp*) (0%, 50%, 75% e 100%). O primeiro ano de colheita da cana-de-açúcar e quatro anos de colheita consecutivas de 2013 a 2017. O resultado a tolerância à perda de solo de $4,3 \text{ Mg ha}^{-1}$ supera a taxa mínima em 40 % da região, resultando em uma perda total de solo de ~ 6 milhões Mg ano^{-1} . Nossos achados sugerem que a produção de palha de cana-de-açúcar não tem sido suficiente para proteger a perda de solo contra a erosão hídrica. Assim, a remoção da palha é inviável a menos que práticas alternativas de conservação sejam adotadas, como preparo mínimo do solo, curvas de nível, terraços e outras técnicas que favoreçam o aumento do teor de matéria orgânica e cátions floclulantes do solo. Esta pesquisa identifica áreas propensa à erosão que imediatamente requer um guia de desenvolvimento de terras sustentável para restaurar e reabilitar os serviços ecossistêmicos vulneráveis. O método espaço-temporal aplicado nesse trabalho pode identificar áreas propensas à degradação do solo e a expansão das terras agrícolas. Essas informações podem orientar proprietários e formuladores de políticas a aplicar técnicas de conservação mais avançadas de acordo com a variação específica do local.

Palavras-chave: Degradação do solo, RUSLE; sensoriamento remoto; resíduos agrícolas; palha; cana-de-açúcar; bioenergia; uso sustentável do solo.

ABSTRACT

Intensive cropland expansion for an increasing population has driven soil degradation worldwide. Modeling how agroecosystems respond to variations in soil attributes, relief, and crop management dynamics can guide soil conservation. This research presents a new approach to evaluate soil loss by water erosion in cropland using the RUSLE model and time series remotely-sensed environmental, agricultural and anthropic variables in the Southeast region of São Paulo State, Brazil. The availability of the open-access satellite images of Tropical Rainfall Measuring Mission (TRMM) and Landsat satellite images provided ten years of rainfall data and 35 years of exposed soil surface. The bare soil surface and agricultural land use were extracted and the multi-temporal rainfall erosivity were assessed. We predict soil maps' attributes (texture and organic matter) through innovative soil spectroscopy techniques to assess soil erodibility and soil loss tolerance. Erosivity, erodibility, and topography obtained by the Earth observations were adopted to estimate soil erosion in four scenarios of sugarcane (*Saccharum spp*) residue coverage (0%, 50%, 75%, and 100%) in five years of the sugarcane cycle, the first year of sugarcane harvest and four subsequently harvesting years from 2013 to 2017. Soil loss tolerance means 4.3 Mg ha^{-1} exceeds the minimum rate in 40 % of the region, resulting in a total soil loss of ~ 6 million Mg yr^{-1} under total coverage management (7 Mg ha^{-1}). Our findings suggest that sugarcane straw production has not been sufficient to protect the soil loss against water erosion. Thus, straw removal is unfeasible unless alternative conservation practices are adopted, such as minimum soil tillage, contour lines, terracing and other techniques that favor increases in organic matter content and soil flocculating cations. This research also identifies a spatiotemporal erosion-prone area that requests an immediately sustainable land development guide to restore and rehabilitate the vulnerable ecosystem service. The high-resolution spatially distribution method provided can identify soil degradation prone areas and the cropland expansion frequency. This information may guide farms and the policymakers for a better request of conservation practices according to site-specific management variation.

Keywords: Soil degradation; RUSLE; remote sensing; crop residue; sugarcane; sugar cane straw; bioenergy; sustainable land use.

SUMMARY

CHAPTER 1. GENERAL INTRODUCTION.....	11
1.2 REFERENCES	15
CHAPTER 2 SOIL EROSION SATELLITE-BASED ESTIMATION IN CROPLAND FOR SOIL CONSERVATION	17
2.1 INTRODUCTION.....	18
2.2 MATERIAL AND METHODS.....	21
2.2.1 SITE DESCRIPTION AND SUGARCANE CYCLE	21
2.2.2 SOIL SAMPLING.....	22
2.2.3 PARAMETRIZATION OF SOIL LOSS BY WATER EROSION	23
2.2.3.1 <i>Rainfall Erosivity Factor (R)</i>	25
2.2.3.2 <i>Soil Erodibility Factor (K)</i>	26
2.2.3.3 <i>Slope Length and Steepness Factor (LS)</i>	28
2.2.3.4 <i>Control Practice Factor (P)</i>	29
2.2.3.5 <i>Cover Management Factor (C)</i>	29
2.2.4 SOIL LOSS TOLERANCE	31
2.3. RESULTS.....	31
2.3.1 SOIL DEGRADATION SPATIAL ANALYSES ESTIMATED BY RUSLE	32
2.3.1.1 <i>Rainfall erosivity factor</i>	32
2.3.1.2 <i>Soil erodibility factor obtained from the digital soil attributes mapping</i>	33
2.3.1.3 <i>The topographic parameters and control practice</i>	38
2.3.1.4 <i>Cover management factor</i>	39
2.3.2 SOIL LOSS IN AGRICULTURAL REGIONS	40
2.4 DISCUSSION.....	42
2.5 CONCLUSION.....	46
2.6 REFERENCES	47
CHAPTER 3. FINAL CONSIDERATIONS.....	55
CHAPTER 4. GENERAL REFERENCES.....	60
APPENDIX	61

CHAPTER 1. GENERAL INTRODUCTION

Soil is a crucial natural resource vital to the planet's functioning. It interacts with the atmosphere, biosphere, hydrosphere, and lithosphere (BRADY; WEIL, 2008), supporting food, fiber, bioenergy production, carbon storage, biodiversity, water filtration, and nutrient transformation (BANWART, 2011).

The world's soil is facing significant degradation. Some soil types are in danger of substantial loss or complete extinction due to various factors, such as agriculture and urbanization pressure, leading to soil loss, erosion, salination, and pollution (AMUNDSON; GUO; GONG, 2003). Soil losses in some locations worldwide are losing soil 100 times faster than the rate of soil formation (BANWART, 2011). Why are we facing this scenario if we have so much soil information worldwide?

The soil diversity has not been assigned. Understanding soil diversity and its ability to support soil management is fundamental to management practices regarding fertilizer application, the design of field research programs, and other soil-dependent activities (GALLO et al., 2018). Therefore, soil conservation practices such as conservation tillage, crop rotation, cover cropping, agroforestry, and soil amendments have been developed to mitigate soil degradation and promote sustainable land management (FAO, 2015).

Soil conservation is critical to achieving the Sustainable Development Goals (SDGs) and the Paris Agreement on climate change. It contributes to food security, climate resilience, and environmental sustainability (LORENZ; LAL; EHLERS, 2019). The SDGs encompass a universal call to action by 2030 to eradicate hunger, poverty, safeguard the planet, and foster global peace and prosperity, echoing their urgency (IPCC, 2019).

Scaling large areas in space and time is no doubt challenging, given the time-consuming and high-cost data acquisition processes required to capture the multifaceted climatic and abiotic ecological factors such as soil characteristics and topography, land use, and land management practices (CERVI et al., 2020). Moreover, land use change does not occur linearly over time, with various factors influencing land rights in different places, such as the political economy and legal situations (IPBES, 2018b).

Multitemporal satellite imagery provides a powerful tool that enables soil information collection on a global scale. It is important for estimating soil erosion and identifying areas at risk of soil loss. The remote sensing technique is handy in extensive agricultural regions, as it enables monitoring large areas of soil spatial variability and identifying surfaces of bare soil frequency over time with minimal cost (DEMATTE et al., 2020b).

A multitude of academic papers have utilized remote sensing to assess land dynamics and soil conservation efforts. In their study, Schultz et al. (2015) applied the proposed approach to a sub-tropical study site in Southeastern Brazil, using a multi-temporal Landsat 8 image as input data. They also incorporated training samples from field visits and very high-resolution (VHR) RapidEye photo-interpretation. The results achieve an overall accuracy (OA) of 80% on pixel-wise classification of five crop classes including, sugarcane, soybean, cassava, and peanut.

The significance of soil conservation in water supply systems is exemplified by the Cantareira System, catering to São Paulo's Metropolitan Region. Lense et al. (2023) employed the RUSLE model, Geographic Information System (GIS), and Remote Sensing to model soil loss and sediment production. The findings underscore the impact of climate change-driven silting on the system, with approximately 3 million Mg of soil loss annually impacting water bodies and critical resource sustainability. Although most of the system maintains tolerable soil loss, about a third faces water and soil resource sustainability challenges. Sustainable solutions, including conservation practices, are essential to maintain the viability of this vital water network.

In Brazil's Cerrado biome, Vieira et al. (2021) utilized the decision tree method and Normalized Difference Vegetation Index (NDVI) derived indices from 1985 to 2018 to predict degradation patterns resulting from agricultural expansion. Their findings highlight approximately 0.63% of the study region experiencing strong degradation signs, primarily in pastures and grasslands, with both low and high soil resilience areas impacted, often influenced by fire. The intricate interplay of factors underscores the urgency of conservation and restoration strategies.

Falcão et al. (2020) utilized a comprehensive approach integrating various data sources, including DEM and Sentinel-2B imagery, to estimate soil erosion within the Brazilian semiarid region. Their results underscore a moderate yet significant mean soil loss, emphasizing the interplay of factors such as soil erodibility and land cover in shaping degradation patterns.

Longato et al. (2019) present a pioneering approach in remote sensing, using data to identify marginal lands for wood biomass production. In Italy's Rovigo province, they classified marginal lands using the Soil Adjusted Vegetation Index (SAVI), unveiling potential trade-offs and synergies between wood crops, food production, and Ecosystem Services (ES). The findings highlight the potential for bioenergy generation while enhancing ES, suggesting an avenue for enhancing the multifunctionality of agricultural landscapes.

These studies collectively underscore the indispensability of remote sensing in identifying regions susceptible to soil degradation and guiding effective conservation strategies.

The research presented in this study draws inspiration from a broader effort to promote the use of crop residues for bioenergy production, focusing on sugarcane straw. Straw is a valuable biomass feedstock for bioenergy production in Brazil (CARVALHO et al., 2016). As a byproduct of sugarcane harvesting, the straw can be abundant in many sugarcane-growing regions around the world. Sugarcane is a globally cultivated crop with leading producers in Brazil, India and China. With the increasing demand for renewable energy sources, straw has emerged as a promising feedstock due to its high lignocellulosic content and versatility in converting to different forms of energy, such as electricity, heat, and biofuel (CERVI et al., 2020). However, soil erosion can be a significant concern in areas where sugarcane straw is removed. Straw removal can negatively impact soil health, decreasing crop yields and productivity (BORDONAL et al., 2018; CHERUBIN et al., 2018)

One approach to using straw for soil conservation is using the residues produced as a cover crop to reduce erosion, protect the soil surface, promote soil moisture retention, and contribute to the soil's organic matter content (TENELLI et al., 2019c). The sustainable management of sugarcane straw for soil conservation and bioenergy production requires understanding the optimal amount of sugarcane straw left on the soil.

In this context, we were motivated to investigate sugarcane straw sustainable management for soil conservation, a previous analysis for straw removal using multitemporal satellite images and remote sensing data (Figure 1) in the Southeastern region of Brazil. The exposed soil was mapped, including texture and organic matter content, and the RUSLE model was used to estimate soil loss by water erosion. To evaluate the impacts of straw removal on soil erosion, we simulated four different scenarios with varying straw coverage rates of 0%, 50%, 75%, and 100% over five years (2013 to 2017).

We have provided spatiotemporal erosion-prone information, highlighting the urgent need for a sustainable land development guide. Our findings emphasize the importance of balancing the use of sugarcane straw for bioenergy production while mitigating soil erosion to preserve soil health and maintain agricultural productivity.

Southeast Brazil is renowned for its rich biodiversity and significant agricultural activities. However, intensive land use and deforestation have led to soil degradation and environmental concerns. Leveraging remote sensing, particularly multitemporal satellite imagery, offers a viable solution to monitor and mitigate soil degradation while exploring bioenergy prospects in the region.

The thesis was structured into three chapters, starting with an introduction to soil concerns of residue removal for the bioenergy industry. The second chapter evaluated spatial

and temporal patterns of soil loss in sugarcane yield using an innovative multitemporal remote sensing data technique. Finally, the third chapter summarized the study's findings and presented directions for future research.

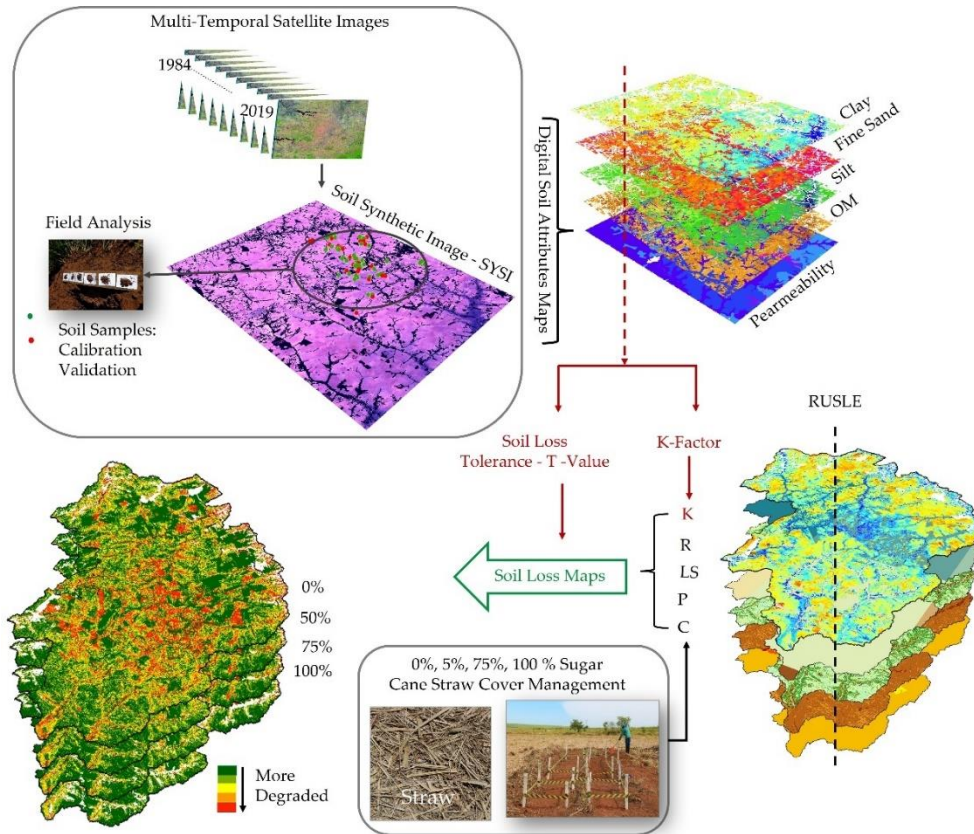


Figure 1. This flowchart provides an overview of the comprehensive approach used to evaluate the effectiveness of sugarcane straw management strategies on soil conservation. First, multitemporal satellite images are combined with field research data to generate a map of the bare soil surface, referred to as the Soil Synthetic Image. Remote sensing techniques are then applied to estimate soil attributes from this image, resulting in digital soil attribute maps. These digital soil attribute maps are utilized in the Revised Universal Soil Loss Equation (RUSLE) model and Soil Tolerance simulations, which assess the impact of different sugarcane straw management scenarios on soil loss. The final map generated from these simulations highlights areas more susceptible to soil erosion and degradation due to poor management practices. The resulting maps can aid in implementing sustainable land management practices to mitigate soil erosion and promote soil health.

1.2 REFERENCES

- AMUNDSON, R.; GUO, Y.; GONG, P. Soil diversity and land use in the United States. *Ecosystems*, v. 6, n. 5, p. 470–482, ago. 2003.
- BANWART, S. Save our soil. *Nature*, v. 474, p. 151–152, 2011.
- BORDONAL, R. DE O. et al. Sustainability of sugarcane production in Brazil. A review. *Agronomy for Sustainable Development*, v. 38, n. 2, p. 13, 27 abr. 2018.
- BRADY, N. C.; WEIL, R. R. *The Nature and Properties of Soils*. 14. ed. New Jersey: Pearson, 2008.
- CARVALHO, J. L. N. et al. Agronomic and environmental implications of sugarcane straw removal : a major review. *Bioenergy Research*, p. 1–16, 2016.
- CERVI, W. R. et al. Mapping the environmental and techno-economic potential of biojet fuel production from biomass residues in Brazil. *Biofuels, Bioproducts and Biorefining*, p. 1–23, 2020.
- CHERUBIN, M. R. et al. Crop residue harvest for bioenergy production and its implications on soil functioning and plant growth: A review. *Scientia Agricola*, v. 75, n. 3, p. 255–272, maio 2018.
- Falcão, C. J. L. M., Duarte, S. M. de A., & da Silva Veloso, A. (2020). Estimating potential soil sheet Erosion in a Brazilian semiarid county using USLE, GIS, and remote sensing data. *Environmental Monitoring and Assessment*, 192(1). <https://doi.org/10.1007/s10661-019-7955-5>.
- FAO. Status of the World's Soil Resources. Food and Agriculture Organization of the United Nations, 2015.
- GALLO, B. et al. Multi-Temporal Satellite Images on Topsoil Attribute Quantification and the Relationship with Soil Classes and Geology. *Remote Sensing*, v. 10, n. 10, p. 1571, 1 out. 2018.
- IPCC. *Climate Change and Land - IPCC Special Report on Climate 21 Change, Desertification, Land Degradation, Sustainable Land Management, Food Security, and Greenhouse gas fluxes in Terrestrial Ecosystems*. [s.l: s.n.].
- Lense, G. H. E., Lämmle, L., Ayer, J. E. B., Lama, G. F. C., Rubira, F. G., & Mincato, R. L. (2023). Modeling of Soil Loss by Water Erosion and Its Impacts on the Cantareira System, Brazil. *Water (Switzerland)*, 15(8). <https://doi.org/10.3390/w15081490>.
- Longato, D., Gaglio, M., Boschetti, M., & Gissi, E. (2019). Bioenergy and ecosystem services trade-offs and synergies in marginal agricultural lands: A remote-sensing-based

assessment method. *Journal of Cleaner Production*, 237. <https://doi.org/10.1016/j.jclepro.2019.117672>.

LORENZ, K.; LAL, R.; EHLERS, K. Soil organic carbon stock as an indicator for monitoring land and soil degradation in relation to United Nations' Sustainable Development Goals. *Land Degradation & Development*, v. 30, n. 7, p. 824–838, 30 abr. 2019.

Schultz, B., Immitzer, M., Formaggio, A. R., Sanches, I. D. A., Luiz, A. J. B., & Atzberger, C. (2015). Self-guided segmentation and classification of multi-temporal Landsat 8 images for crop type mapping in Southeastern Brazil. *Remote Sensing*, 7(11), 14482–14508. <https://doi.org/10.3390/rs71114482>.

TENELLI, S. et al. Can reduced tillage sustain sugarcane yield and soil carbon if straw is removed? *BioEnergy Research*, v. 12, n. 4, p. 764–777, 26 dez. 2019.

Vieira, R. M. da S. P., Tomasella, J., Barbosa, A. A., Polizel, S. P., Ometto, J. P. H. B., Santos, F. C., Ferreira, Y. da C., & Toledo, P. M. de. (2021). Land degradation mapping in the MATOPIBA region (Brazil) using remote sensing data and decision-tree analysis. *Science of the Total Environment*, 782. <https://doi.org/10.1016/j.scitotenv.2021.146900>.

CHAPTER 2 SOIL EROSION SATELLITE-BASED ESTIMATION IN CROPLAND FOR SOIL CONSERVATION

(Remote Sens. 2023, 15(1), 20; <https://doi.org/10.3390/rs15010020>)

Bruna Cristina Gallo^{1,2}, Paulo Sérgio Graziano Magalhães³, *José A. M. Demattê⁴, Walter Rossi Cervi^{1,5}, João Luís Nunes Carvalho², Leandro Carneiro Barbosa², Henrique Belinasso⁴, Danilo César de Mello⁶, Gustavo Vieira Veloso⁶, Marcelo Rodrigo Alves⁷, Elpídio Inácio Fernandes-Filho⁶, Márcio Rocha Francelino⁶, Carlos Ernesto Gonçalves Reynaud Schaefer⁶;

¹ University of Campinas, Interdisciplinary Ph.D. Program in Bioenergy, Campinas, SP, Brazil; gallo.bruna@gmail.com;

² Brazilian Biorenewables National Laboratory (LNBR), Brazilian Center of Energy and Material Research (CNPEN), Campinas, SP, Brazil; joao.carvalho@lnbr.cnpem.br; leandrobarbosaagro@gmail.com

³ University of Campinas, Interdisciplinary Center of Energy Planning, Campinas, SP, Brazil; graziano@g.unicamp.br

⁴ Department of Soil Science, Luiz de Queiroz College of Agriculture, University of São Paulo, Piracicaba, Brazil; jamdemat@usp.br; henriquebellinasso@usp.br

⁵ Utrecht University, Copernicus Institute of Sustainable Development, Utrecht, The Netherlands; waltercervi@gmail.com

⁶ Department of Soil Science, Federal University of Viçosa, Brazil; daniloc.demello@gmail.com; gustavo.v.veloso@gmail.com; elpidio@ufv.br; marcio.francelino@ufv.br; carlos.schaefer@ufv.br

⁷ Department of Environment and Regional Development, University of West São Paulo (UNOESTE), Rod. Raposo Tavares, km 572 - Limoeiro, Presidente Prudente - SP, 19067-175, Brazil; marceloalves@unoeste.br

* Correspondence: jamdemat@usp.br

Abstract: Intensive cropland expansion for an increasing population has driven soil degradation worldwide. Modeling how agroecosystems respond to variations in soil attributes, relief, and crop management dynamics can guide soil conservation. This research presents a new approach to evaluate soil loss by water erosion in cropland using the RUSLE model and time series remotely sensed environmental, agricultural and anthropic variables in the Southeast region of São Paulo State, Brazil. The availability of the open-access satellite images of

Tropical Rainfall Measuring Mission (TRMM) and Landsat satellite images provided ten years of rainfall data and 35 years of exposed soil surface. The bare soil surface and agricultural land use were extracted and the multi-temporal rainfall erosivity were assessed. We predict soil maps' attributes (texture and organic matter) through innovative soil spectroscopy techniques to assess soil erodibility and soil loss tolerance. Erosivity, erodibility, and topography obtained by the Earth observations were adopted to estimate soil erosion in four scenarios of sugarcane (*Saccharum spp*) residue coverage (0%, 50%, 75%, and 100%) in five years of the sugarcane cycle, the first year of sugarcane harvest and four subsequently harvesting years from 2013 to 2017. Soil loss tolerance means 4.3 Mg ha⁻¹ exceeds the minimum rate in 40 % of the region has the average of 4.3 Mg ha⁻¹ soil loss, resulting in a total soil loss of ~ 6 million Mg yr⁻¹ under total coverage management (7 Mg ha⁻¹). Our findings suggest that sugarcane straw production has not been sufficient to protect the soil loss against water erosion. Thus, straw removal is unfeasible unless alternative conservation practices are adopted, such as minimum soil tillage, contour lines, terracing and other techniques that favor increases in organic matter content and soil flocculating cations. This research also identifies a spatiotemporal erosion-prone area that requests an immediately sustainable land development guide to restore and rehabilitate the vulnerable ecosystem service. The high-resolution spatially distribution method provided can identify soil degradation prone areas and the cropland expansion frequency. This information may guide farms and the policymakers for a better request of conservation practices according to site-specific management variation.

Keywords: Soil Degradation, RUSLE, Remote Sensing, Crop Residue, Bioenergy, Sustainable Land Use

2.1 INTRODUCTION

One-third of global land is occupied by livestock (21%) and agriculture (12%) (OLSSON et al., 2019). The increasing demand of a growing population projected to reach 9.6 billion by 2050 from the current 7.7 billion (PANAGOS; BORRELLI; ROBINSON, 2020) has put pressure on the Earth's land for food, natural resources, and climate change and created new challenges between humanity and the world's fertile soil resources.

Soil erosion rates caused by the immense expansion of cropland areas have exceeded the rate at which soil is formed by one to two orders of magnitude (MONTGOMERY, 2012). The process of soil erosion usually involves detachment, breakdown, transport, redistribution and deposition of sediments (LAL, 2003). Soil erosion globally has resulted in around 25 to 40

billion tons of increased sediment every year (PANAGOS; BORRELLI; ROBINSON, 2020). Land-use change to cropland is responsible for ~80% of the erosion increase. The highest soil erosion occurs in the least developed countries due to accelerated soil erosion driven by land-use change and poor land management. On the other hand, these countries have the highest potential for soil erosion reduction by conservation agriculture adoption (BORRELLI et al., 2017).

Sustainable land management (SLM) is treated as an effective land degradation reduction method to achieve the Sustainable Development Goals (SDGs) regarding food, health, water, climate, and land management (LORENZ; LAL; EHLERS, 2019a). SDGs are a global call to end hunger and poverty, protect the planet, and ensure peace and poverty for all by 2030. Despite the SLM's importance for land and soil degradation, identifying large soil management scaling areas in space and time are challenging due to time-consuming and high cost for data acquisition of the complex climatic, abiotic ecological factors (i.e., soil characteristics and topography), type of land use and land management practices (i.e., tillage and crop rotation). Land-use change does not occur linearly over time since land rights vary in places and are dependent on the political-economic and legal situation (IPBES, 2018).

The Universal Soil Loss Equation (USLE) (WISCHMEIER; SMITH, 1978) and its revised version (RUSLE) (RENARD et al., 1997) are the most used empirical models to estimate soil erosion driven by water globally. It aims to guide conservation planning and supports the planners to evaluate and predict soil erosion rate for each of several alternative combinations of cropping systems and management techniques on any site within the specified limits. The RUSLE equation integrates erosivity, erodibility, topography, cover management, and support practice factors. Further, it considers soil loss tolerance, which ponders the productivity loss due to erosion with the rate of soil formation from parent material, the role of topsoil formation, loss of nutrients and the cost to replace them (RENARD et al., 1997).

Remote Sensing (RS) linked with Geographic Information System (GIS) combined in RUSLE provide data to compute soil erosion with better spatial coverage and accuracy with reasonable costs (OSTOVARI et al., 2017). The soil spectroscopy advent overcomes the lack of reliable soil data that can be applied to the least developed economies. This method along with the Earth observation based data can be used to assess soil erodibility factor based on the environmental soil service (organic matter and mineral composition) with the spectral reflectance data (OSTOVARI et al., 2017; TENG et al., 2016).

Southeast Brazil is the core of sugarcane production with about 5 million hectares in the 2019/2020 season (62% of the national production) (WALTER et al., 2016). It was estimated

that 600 million Mg yr⁻¹ of annual rainfall soil erosion loss occurs annually in this region (DE OR MEDEIROS et al., 2016). Sugarcane crop in southern Brazil requires a large amount of land to produce biofuels, sugar and electricity. In general, sugarcane production is based on conventional tillage using green mechanized harvesting every year, with a replanting period every five years. The transition from a burned to green harvest system resulted in the maintenance of a large amount of sugarcane straw on the soil surface (CARVALHO et al., 2016b). The thick layer of straw (ranging from 10 to 20 Mg tons ha⁻¹) covering the soil after harvesting, resulted in several benefits, such as nutrient cycling (CHERUBIN et al., 2019), carbon storage (TENELLI et al., 2019b), better soil physical and biological conditions (CASTIONI et al., 2019; MENANDRO et al., 2019) and control against erosion processes (MARTINS-FILHO et al., 2009). However, although straw covers results in several ecosystem benefits, Brazil's more recent sugarcane sector has shown interest in removing part of this crop's residue for bioenergy production, which would lead to increased soil degradation in sugarcane fields (FRANCO et al., 2013).

There is a tenuous line between soil degradation and sustainable land management in cropland. In sugarcane fields, straw is an essential source of soil conservation because it benefits soil functioning, e.g., erosion protection cover, soil temperature amplitude reduction, biological activity increasing (CARVALHO et al., 2013). Studies have demonstrated that maintaining 7 to 10 Mg tons ha⁻¹ of straw is enough to cover 100% of the area prevailing the crop's agronomic benefits (JONES et al., 2017; SILVA et al., 2019). It suggested that if straw yield exceeds this amount, it may be used as feedstock for Brazil's bioenergy demand (bioelectricity and cellulosic ethanol).

This paper presents a new approach to evaluate spatial and temporal patterns of soil loss and the impacts of straw removal in the Southeastern part of Brazil by integrating environmental variables with the cropland management dataset, field data, RS and GIS data in the RUSLE model. A modern multi-temporal satellite-based estimation method was conducted to assess soil properties, spatial patterns of agricultural land use over the last three decades, and rainfall data in the last decade. Four soil loss scenarios have been assessed by simulation with four different straw coverage rates of about 0%, 50%, 75% and 100%, respectively, in five years of the sugarcane cycle (2013-2017) to enlighten the impacts of straw removal changes on soil erosion.

The main novelties of this research are related to soil erodibility parameters of RUSLE and soil loss tolerance obtained by soil attributes maps (texture and organic matter) through bare soil spectroscopy technique (Synthetic Soil Image). This method combines and use

Revised Universal Soil Loss Equation (RUSLE) model associated with a time series remotely-sensed data estimate soil loss by water erosion in cropland.

2.2 MATERIAL AND METHODS

2.2.1 Site description and sugarcane cycle

We evaluate soil erosion of 500 km² of agricultural sugarcane land-use area, located in the Southeastern part of Brazil, west of São Paulo State (Fig. 2.1a). The erosion processes in this region may deliver sediments to the nearby rivers. Therefore, we expanded soil erosion estimations into 13 sub-basins (~1,600 km²) based on the streamflow in order to have a multi-perspective overview of the possible off-site effects of soil erosion on the hydrological ecosystem (Fig. 2.2a).

The region is classified as Tropical with dry winter (May-September). The average annual rainfall is 1391 mm yr⁻¹, and the average annual temperature is 24°C (BORDONAL et al., 2018). The landscape is gently undulating and rolling uplands, with slopes ranging between 0 and 28%. The predominance of sandy-mudstone parental material (PERROTTA et al., 2005) characterizes the soils' sandy/loam texture dominance. Sheet and interrill are preponderating types of erosion in the study site (Fig 2.1b), but gully erosion sites are common, especially in ascending terrain (Fig 2.1c).

The sugarcane cycle comprises five years: the plant cane harvest and four subsequent harvesting years (ratoons) (Fig 2.2). Conventional tillage operations are the most common practices during the plant cane stage and the replanting period, which lies in glyphosate application, subsoiling, plowing, harrowing with physical, chemical, and or biological corrections. Conventional tillage is the most critical period due to the expose soil period until the crop canopy closure (three to six months later) causing erosion. In areas cultivated with sugarcane, the main attributes of the terrain that contribute to erosion are extreme weather events such as high intensity and volume of rainfall, soil exposure associated with sloping reliefs. So, the harvest period occurs every year or 18 months, the maintenance of the straw in the field reduces the risk of soil erosion at this step.

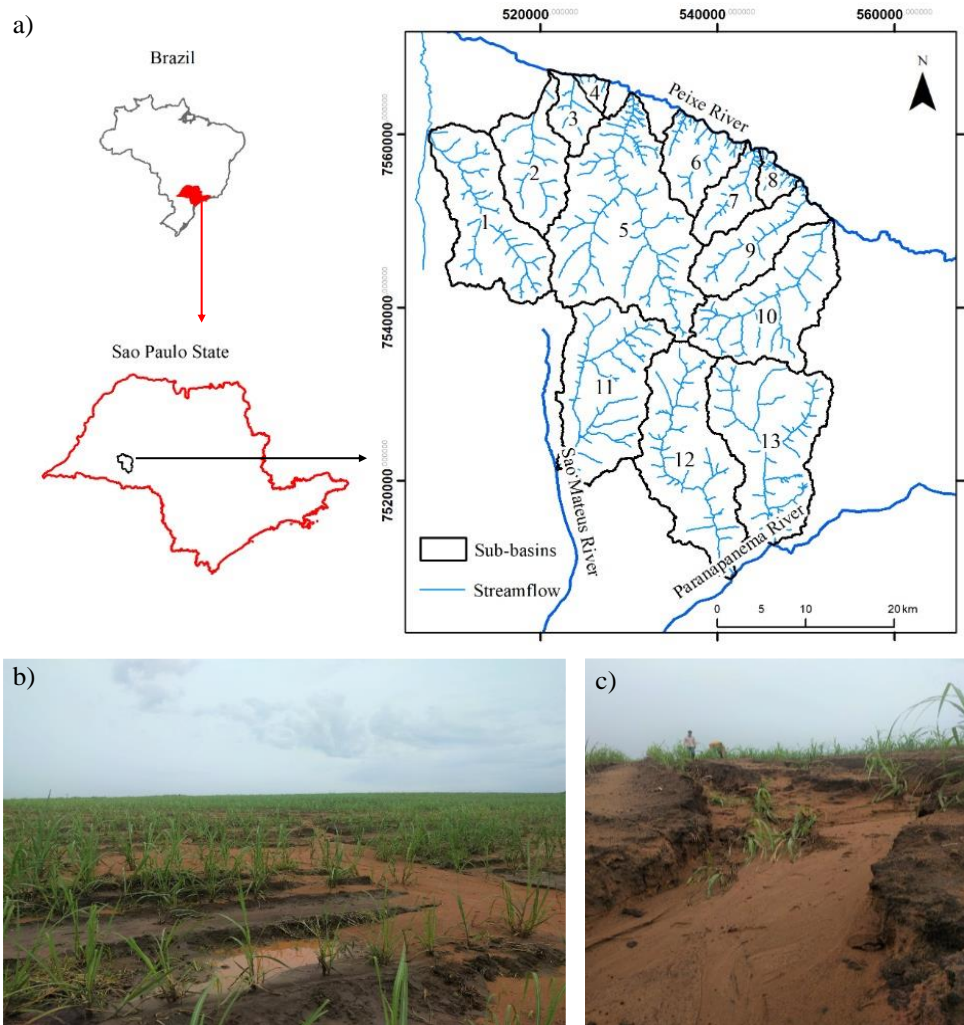


Figure 2.1. a) Study Location; b) Sheet and interrill erosion process and c) gully erosion development during the rainy season in the beginning of the plant cane under conventional tillage.

2.2.2 Soil sampling

Sixty-Seven topsoil (Epipedon) samples were collected randomly, 20% of the soil samples validated the soil erodibility maps generated from Remote Sensing. The soil samples brought to the laboratory oven-dried for 48h at 50 °C, grounded and sieved (2 mm mesh) to analyze soil organic carbon and particle size properties according to the (EMBRAPA, 2017). The main soil classes found in the study site, according to World Reference Base for Soil Resources (WRB) (IUSS WORKING GROUP WRB, 2015) were: Gleysols, Ferralsols, Lixisols, Leptosols and Arenosols.

2.2.3 Parametrization of soil loss by water erosion

Multi-temporal satellite image and field observations assessment provide soil loss estimation. The figure 2.2 demonstrates the general flowchart of the methodology to obtain soil loss.

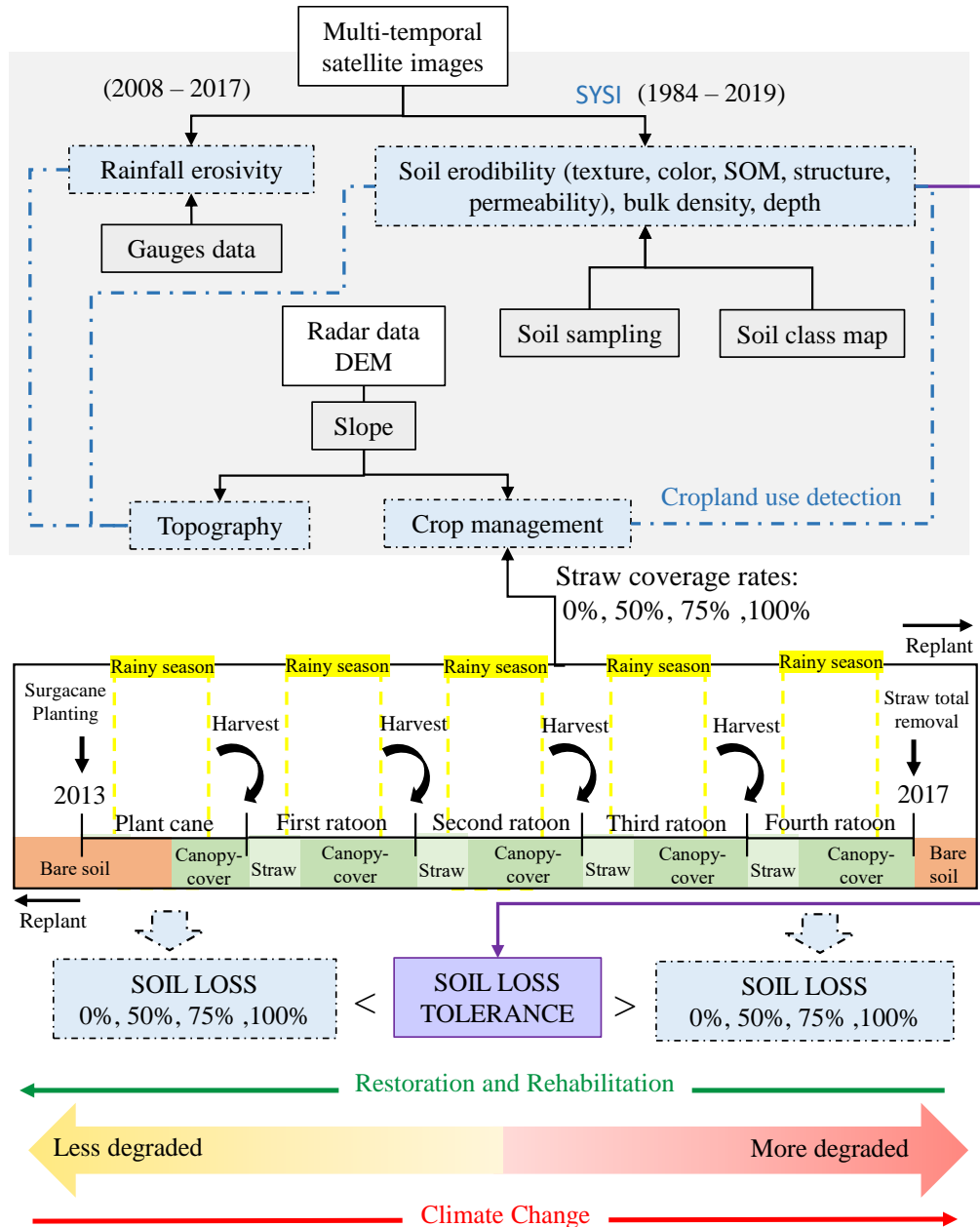


Figure 2.2 Flowchart of the methodology to obtain soil loss. The multi-temporal satellite image and field observations data used to estimated and validated rainfall erosivity and soil erodibility, a digital elevation model used to derive the slope. The Synthetic Soil Image (SYSI) technique based on remote sensing and soil spectroscopy derived soil attributes maps to calculate soil erodibility, soil loss tolerance and detect the cropland use spatial patterns. The environmental variables (rainfall, erodibility and topography) associate with the cropland

patterns and the cropland management dataset (five years of the sugarcane cycle) under different amounts of straw (0%, 50%, 75%, and 100%) estimate soil loss. Soil loss higher than the tolerance indicate high land degradation that contribute to increase climate change crises, while lower indicate restoring and rehabilitation of the ecosystem.

The Revised Universal Soil Loss Equation (RUSLE) (Eq. 1) MENDELEY CITATION PLACEHOLDER 27 implemented in Geographic Information System (GIS) was used to assess the soil erosion rate (Table 2.1 and Fig 2.1). Soil losses by water erosion refer to the amount of sediment that reaches the end of a specified area (cell) on a hillslope (BORRELLI et al., 2017). Using a GIS raster scheme means that each cell is independent of the others. Thus, soil erosion is not routed downslope across each cell from hill(BENAVIDEZ et al., 2018)slopes to the sink area or the riverine systems. The RUSLE model does not capture gullying and other geomorphic processes (i.e., mudflows, landslides and tillage erosion) (BORRELLI et al., 2018). However, it indicates the soil loss rate at which gully erosion might be expected to begin (RENARD et al., 1997).

$$\text{Soil Loss} = R * K * LS * C * P \text{ (Eq. 1)}$$

The detachment-limited model outputs the mass of soil lost per unit area and time ($\text{Mg ha}^{-1} \text{ yr}^{-1}$). Sheet, inter rill and rill erosion processes are given by the multiplication of six parameters: rainfall erosivity (R-Factor in $\text{MJ mm}^{-1} \text{ h}^{-1} \text{ y}^{-1}$), soil erodibility (K-Factor in $\text{tons. h. MJ}^{-1} \text{ mm}^{-1}$), slope length (L-Factor in meters), slope steepness (S-Factor in percentage), cropping system (C-Factor), and erosion control practice (P-factor). C and P factors are dimensionless (Table 1). The spatial resolutions range from 30 m to 25 km, the parameters were resampled to 30 x 30 m cell size to model soil loss as the final output.

Soil loss tolerance threshold (T-value) indicates the maximum rate of soil erosion that can occur and still permits crop productivity to be sustained economically (RENARD et al., 1997; WISCHMEIER; SMITH, 1978). T value according to (“U.S. Department of Agriculture, Agricultural Research Service and Soil Conservation Service”, 1956) is estimated by: (1) soil thickness; (2) soil formation rate; (3) guidelines of the USDA-NRCS; and (4) productivity index. In addition, T value for a specific soil is a function of: the rate of soil formation from parent material; the rate of topsoil formation from subsoil; reduction of crop yield by erosion; soil depth; changes in soil attributes favorable for plant growth; loss of plant nutrients by erosion; the likelihood of rill and gully formation; sediment deposition problems within a field;

sediment delivery from the erosion site and; the availability of feasibility, economic, culturally and socially in addition to soil conservation practices (“U.S. Department of Agriculture, Agricultural Research Service and Soil Conservation Service”, 1956). Cropping management practices with the predicted soil loss rate less than the T-value rate may be projected to deliver less soil degradation (Fig 2.2). Thus, sustainable land management practices can reduce the risk of land degradation and mitigate the climate change impacts by promoting restoration and rehabilitation of the ecosystems, for example, by improving their carbon stock (OLSSON et al., 2019).

Table 2.1. Synthesis of the RUSLE spatial dataset required to map soil loss by water erosion

Factor	Environmental dataset	Tools/Method	Variability	Spatial dataset	Resolution/ Map Scale
Rainfall (R-Factor)	Average Monthly/Annual Rainfall	Google Engine, Literature/MFI ¹ /EI ₃₀ ²	Spatiotemporal (10 years)	TRMM ³	25 km
Soil (K-Factor)	Texture, Organic Matter, Bulk Density	Google Engine/SYSI ⁴ and R program/ DSM ⁵	Spatiotemporal (35 years)	Landsat	30 m
	Permeability and Structure Code	Legacy Soil Maps	Shape	Region Map Local Soil Map	1:250.000 1:50.000
Topography (LS-Factor)	Slope, Flow direction, Flow accumulation	ArcGIS	Spatial	SRTM ⁶	30 m
Management (P-Factor)	Slope and Contour Farming	ArcGIS	Spatial	SRTM ⁶	30 m
(C-Factor)	Land use	Google Engine/SYSI ⁴	spatiotemporal (35years)	Landsat	30 m
	Canopy-cover, Surface-cover, Surface-roughness, Soil moisture	Excel/ Sugarcane Management Combinations ⁷	Shape (5 years)	Cropland Plots	1:50.000

¹MFI: Modified Fournier Index, ²EI₃₀: Erosivity Index, ³TRMM: Tropical Rainfall Measuring Mission, ⁴SYSI: Soil Synthetic Image, ⁵DSM: Digital Soil Map, ⁶SRTM: Shuttle Radar Topographic Mission, ⁷Local, Planting and Tillage Date, Tillage System, Crop Rotation, Straw Management, Sugarcane Cycle, and Management Levels.

2.2.3.1 Rainfall Erosivity Factor (R)

Rainfall erosivity represents the erosive powers of rainfall energy (intensity and duration), a total of rain (volume) and frequency over extended time events. We calculated R-factor using ten years (2008-2017) data of the monthly 3B42 product from the Tropical Rainfall

Measuring Mission (TRMM) Multi-satellite Precipitation Analysis (TMPA). Several studies worldwide have estimated erosivity at fair resolution using the TRMM (TENG et al., 2016; VRIELING; HOEDJES; VAN DER VELDE, 2014; VRIELING; STERK; DE JONG, 2010). This product provides global coverage of precipitation (mm hr^{-1}), with a 3-hour temporal resolution and a 0.25-degree spatial resolution (HUFFMAN et al., 2007).

We performed the Modified Fournier Index (MFI) (Eq. 2) using TRMM products to estimate erosivity factor according to the Erosivity Index (EI_{30}) equations recommended by (MELLO et al., 2013; OLIVEIRA; WENDLAND; NEARING, 2013). The EI_{30} is defined as the product of the maximum rain intensity during a 30-minutes period. There are three main stations relating EI_{30} to MFI that fitted the study site location (Table 2). Our calculated R-Factor is an average of the three erosivity equations. We used data from seven gauges provided by the Water and Electric Energy Department of São Paulo State (DAEE-SP) located towards the study site to validate the R-Factor obtained from TRMM.

$$\text{MFI} = \frac{1}{P} \sum_{i=1}^{12} P_i^2 \quad (\text{Eq. 2})$$

P is the average annual rainfall (mm), and P_i is the average rainfall (mm) in the month i.

Table 2.2 Erosivity equations studies around the study site.

Latitude	Longitude	City/ State	Equation	Authors
22° 37' 0"S	52° 10' 0"W	Teod. Sampaio/SP	$\text{EI}_{30}=106.82+46.96 (\text{MFI})$	(COLODRO et al., 2002)
22° 31' 12"S	47° 2' 40"W	Campinas/SP	$\text{EI}_{30}=68.73 (\text{MFI})^{0.841}$	(LOMBARDI NETO; MOLDENHAUER, 1992)
23° 13' 0"S	49° 14' 0"W	Piraju/SP	$\text{EI}_{30}=72.55 (\text{MFI})^{0.8488}$	(ROQUE; CARVALHO; PRADO, 2001)

EI_{30} : Erosivity Index and MFI: Modified Fournier Index

2.2.3.2 Soil Erodibility Factor (K)

The soil erodibility factor (BENAVIDEZ et al., 2018) represents soil susceptibility to erosion. Soil particle size distribution (clay, fine sand, and silt contents), soil organic matter (SOM) content, soil structure, and profile permeability are the attributes required to estimate K-Factor [27] (Eq. 9) (WISCHMEIER; SMITH, 1978).

$$K = [2.1 * 10^{-4} * M^{1.14} (12-OM) + 3.25 (S-2) + 2.5 (Q-3) / 100] * 0.1317$$

(Eq. 3)

$M = (\% \text{ silt} + \% \text{ fine sand}) * (100 - \% \text{ clay})$. OM is soil organic matter content (%). S is soil structure code (1-4). Q is permeability code (1-6).

Here, the topsoil attributes were spatially modelled using an improved methodology with satellite Bare Soil Composite Image (GALLO et al., 2018) based on a Geospatial Soil Sensing System data-mining algorithm. This algorithm flagged bare surfaces from the collection of historical images and aggregated the spatially bare soil fragments into a synthetic soil image (SYSI) (DEMATTÉ et al., 2018, 2020; SAFANELLI et al., 2020). In this study, we used multi-temporal Landsat satellite images to extract bare soil fragments from 1984 to 2019 and aggregate them, in order to obtain all periods of exposed soil for later creation of a mosaic, which allows viewing the entire area of interest with exposed soil surface. Landsat imagery has the wavelengths (Bands) of Visible (VIS – Blue/Green/Red), Near Infrared (NIR) and Shortwave Infrared (SWIR1 and SWIR 2) with 30 m of spatial resolution and 16 days of temporal resolution.

MID-Infrared and NDVI indexes were used to remove vegetation and crop residue in each image. We used quality bands to mask clouds and shadows. MID-Infrared represents the normalized difference index calculated from Landsat bands SWIR1 and SWIR2, and NDVI defines the normalized difference vegetation index calculated from Landsat bands NIR and Red. MID-Infrared and NDVI threshold combinations of -0.25 to 0.25 and 0.013 to 0.10 were performed. The indexes threshold was determined based on studies related to soil reflectance (DEMATTÉ et al., 2020; SAFANELLI et al., 2020) and field observation. We used quality bands to mask clouds and shadows or pixels with inconsistent values and we choose a filter to use Landsat images with no clouds. The images were aggregated into a single image by the median spectral reflectance value achieving the SYSI of the agricultural spatial patterns from a time interval of 1984 to 2019, with a native spatial (30m) Landsat product. We used Google Earth engine platform to acquire the SYSI algorithm.

We performed a partial least square regression (PLSR) method to predict the digital soil mapping attributes by inputting the multi-temporal spectra data from the SYSI and the field measured soil samples (80 % employed for calibration and the remaining 20 % for validation)

at the R program. The models were evaluated based on the coefficient of determination (R^2), and the root means square error (RMSE).

2.2.3.3 Slope Length and Steepness Factor (LS)

LS-Factor (BENAVIDEZ et al., 2018) describes the effect of the topography on soil erosion. The L-Factor calculates the slope length, and the S-Factor measures the slope steepness. L-Factor represents the distance from the overland flow point of origin to the point where the slope gradient decreases, and water runoff streamed into a channel and deposition starts (PANAGOS; BORRELLI; MEUSBURGER, 2015; WISCHMEIER; SMITH, 1978).

(FOSTER; MEYER; ONSTAD, 1977) identify that S-Factor is not uniform for a whole area; hence, they proposed sub-divide the slope into several segments. Later (DESMET; GOVERS, 1996) extended this approach to a two-dimensional terrain using the unit-contributing area model (Eq. 4 to 6). (RENARD et al., 1997) incorporated this approach into RUSLE with slope gradient concepts of (MCCOOL et al., 1987), and found that soil loss arises faster in slopes that were steeper than 9% (Eq. 7 and 8).

The LS-Factor was derived from a Digital Elevation Model (DEM) product obtained from the Topodata [44], which filled the original Shuttle Radar Topographic Mission (SRTM) 3 arc-second (90 m) data into an interpolated DEM of 1 arc-second (30 m). We calculated the slope length and slope steepness factors at the ArcGIS platform according to (DESMET; GOVERS, 1996; RENARD et al., 1997).

$$L_{i,j} = \frac{(A_{i,j-i,n} + D^2)^{m+1} - (A_{i,j-i,n})^{m+1}}{(D^{m+2}) * (x_{i,j}^m) * (22,13)^m} \quad (\text{Eq. 4})$$

$$m = \frac{\beta}{\beta+1} \quad (\text{Eq.5})$$

$$\beta = \frac{\frac{\sin \theta}{0.0896}}{[0.56+3*(\sin \theta)^{0.8}]} \quad (\text{Eq. 6})$$

$$S = 10.8 * \sin \theta + 0.03, \text{ where slope gradient} < 0.09 \text{ ou } 9\% \quad (\text{Eq.7})$$

$$S = 16.8 * \sin \theta - 0.5, \text{ where slope gradient} \geq 0.09 \quad (\text{Eq. 8})$$

$L_{i,j}$ is the slope length factor for the grid cell with coordinates (i, j). $A_{i,j}$ is an upslope contributing area for the grid cell with coordinates (i, j) (m^2). D is the side length of the grid cell (m). $x_{i,j}$ is a contour length coefficient for the grid cell with coordinates (i, j). m is related to the ratio β of the rill to interill erosion. θ is a gradient of slope in degrees. S is slope steepness.

2.2.3.4 Control Practice Factor (P)

P-Factor measures the ratio of soil loss expected for a specific support conservation practice to the corresponding loss with surface upslope and downslope tillage. The support practices for erosion control usually comprehend contouring, strip-cropping, terracing, and subsurface drainage. These practices influence drainage patterns, runoff velocity, and the direction of water volume concentration (RENARD et al., 1997).

The cropland of the study site mainly applies contour farming in terraces according to the slope gradient. Contour means that farmers implement field practices along contours perpendicular to the normal water flow direction. Consequently, it reduces runoff velocity by increasing the surface roughness providing more time for infiltration (STEVENS et al., 2009), protecting the fertile layer, improving crop yield, increasing income and contributing to the environment. The slope (%) (Table 3) obtained by the DEM (30 m) derived P-Factor for the arable cropland.

Table 2.3. P-Factor for contour support practices for different slope gradients (WISCHMEIER; SMITH, 1978).

Solpe (%)	P-Factor for contouring
1-2	0.6
3-8	0.5
9-12	0.6
13-16	0.7
16-20	0.8
21-25	0.9
> 25	0.95

2.2.3.5 Cover Management Factor (C)

C-Factor comprises the effect of cropping and management practices on soil loss rates; this factor indicates how the management activities will affect the average annual soil and how

the soil erosion potential will be disseminated in time during a conservation plan. C-Factor value for a particular land use type is the weighted average of Soil Loss Ratios (SLRs) that ranges from 0 to 1 (RENARD et al., 1997); as it increases to 1, land use degradation stresses high soil threatens. C-Factor may cause a considerable influence on the erosion calculation, which is defined as the most significant among the RUSLE factors (TANYAŞ; KOLAT; SÜZEN, 2015).

We used a tool developed explicitly for sugarcane crops based on São Paulo State (ROCHA, 2017), and we calibrated it with the sugarcane stalks yield data from the agroindustry plots from 2013 to 2017. This tool enables many combinations of sugarcane system management as input data to obtain SLR subfactors (Eq.9) and to model the average annual C-Factor (Eq. 10). It requires geographic location, date of tillage (month) and tillage growing (winter, year or 18 months), tillage type (conventional, minimum or no-tillage), covers crop (bare soil, bare fallow, and green crop), crop residue management (0% to 100% of crop residues coverage), number of sugarcane cycle, and management level (low, medium and high). In this study, we assumed four cover management scenarios to assign soil loss based on the yield average of the five sugarcane cycles and the ratio of 120 kg of dry matter straw per tons of fresh sugarcane stalk (MENANDRO et al., 2017). The scenarios are classified in: i) no straw coverage rate (0 Mg⁻¹), ii) 50% coverage (3.5 Mg⁻¹), iii) 75% coverage (5.25 Mg⁻¹), and iv) 100 % coverage (7 Mg⁻¹).

SRL is calculated for a given condition using five subfactors and has to be calculated for different periods, as (RENARD et al., 1997) recommended. Each subfactor contains cropping and management variables that affect soil erosion. PLU (Prior-Land Use) expresses the influence on soil erosion of subsurface residual effects from previous crops and the effect of previous crop management practices on soil consolidation. CC (Canopy Cover) indicates the effectiveness of vegetative canopy in reducing the energy of the rainfall striking the soil surface. SC (Surface Cover) affects erosion by reducing the transport capacity of runoff water by causing deposition in ponded areas and decreasing the surface area susceptible to raindrop impact. SR (Surface-Roughness) is a function of the surface's random roughness. SM (Soil-Moisture) influences infiltration, runoff, and soil erosion (RENARD et al., 1997). Here, soil moisture reflects soil field capacity, value 1, due to their intensive condition under the erosive process.

$$SLR = PLU * CC * SC * SR * SM \quad (Eq. 9)$$

$$Factor C = \sum_{i=1}^{12} \frac{SLR_i EI_i}{EI_{annual}} \quad (Eq. 10)$$

EI_i is the rainfall erosivity for the month i ($MJ \text{ mm}^{-1} \text{ h}^{-1} \text{ y}^{-1}$), and EI_{annual} is the annual rainfall erosivity ($MJ \text{ mm}^{-1} \text{ h}^{-1} \text{ yr}^{-1}$).

2.2.4 Soil loss tolerance

Various methods to assess soil loss tolerance have been recommended by soil scientists worldwide; each approach has its assumptions, advantages, and limitations (YANG et al., 2022). Land cover and carbon stocks are the principal indicators to estimate land degradation because they can change rapidly (CHAPPELL et al., 2019). Here, the spatial modeling of soil loss tolerance was estimated based on [53] (Eq. 13), which considers the soil bulk density method obtained in [54] (Eq. 11 and 12) that depends on SOM and soil drained capacity. The soil class map of the agroindustry determined soil drained capacity. The SOM map was estimated by the satellite bare soil surface methodology (Item 2.3.2). Soil depth of 0 - 30m, and the temporal constant founded on the concept that forming 1,000 mm of soil is required 1,000 years (SMITH; STAMEY, 1965) were incorporated in the calculations to obtain T.

$$BD = 1.52 - 0.06 * SOM \text{ (well drained)} \quad (Eq. 11)$$

$$BD = 1.53 - 0.5 * SOM \text{ (imperfectly drained)} \quad (Eq. 12)$$

Where BD is soil bulk density (g cm^{-3}), SOM is organic matter (%)

$$T = \left(\frac{H \times BD}{1,000} \right) * 10,000 \quad (Eq. 13)$$

BD is soil bulk density (kg m^{-3}). SOM is soil organic matter (g kg^{-1}). T is soil loss tolerance ($\text{Mg ha}^{-1} \text{ yr}^{-1}$), H is soil depth (m), 1000 is the temporal constant founded on the concept that forming 1000 mm of soil required 1000 years [53];, and 10,000 factor was applied to transform the data from Mg m^{-2} to Mg ha^{-1} .

2.3. RESULTS

2.3.1 Soil degradation spatial analyses estimated by RUSLE

2.3.1.1 Rainfall erosivity factor

The spatial data average rainfall erosivity calculated represents $6,078.00 \text{ MJ mm}^{-1} \text{ ha}^{-1} \text{ yr}^{-1}$ (Fig. 2.3), which according to (FOSTER et al., 1981; MELLO et al., 2013) indicates strong erosivity, 300% higher than the global average (BORRELLI et al., 2017).

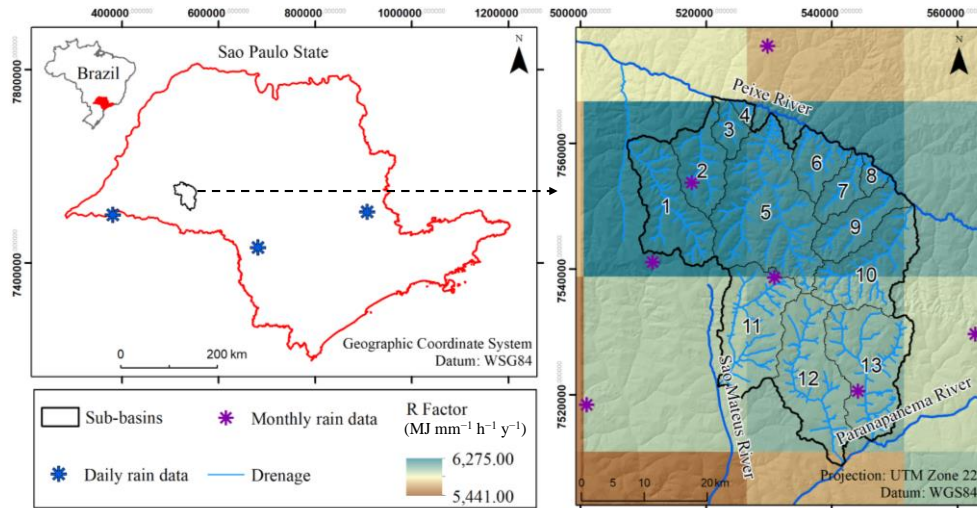


Figure 2.3. The sub-basins' geographic location with the distribution of daily rain data gauges in Sao Paulo State, Brazil and the monthly rain data gauges on the rainfall erosivity (R-Factor) map.

We calculated the R-Factor using TRMM data between 2008 and 2017 and the erosivity equations obtained by the daily rain data as a function of the Modified Fournier Index (MFI) (Fig. 2.3). We compared our estimated R-Factor to that calculated from the monthly rain data gauges covering the sub-basins. In the southeastern part of Brazil, the rainy period marks warm temperatures start in September and ends in May (Fig. 2.4a). The relation has an $R^2 = 0.90$, demonstrating a good correspondence between the values with a close 1:1 relationship (Fig 2.4 b).

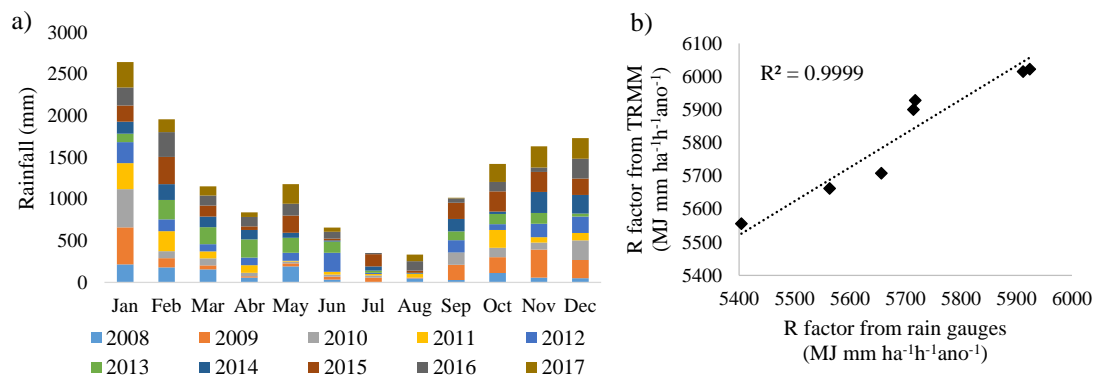


Figure 2.4. a) Annual rainfall distribution from 2008 to 2017 from a station located in the study site, b) R-Factor obtained from the Tropical Rainfall Measuring Mission (TRMM) compared to that obtained from the monthly rain gauges data.

2.3.1.2 Soil erodibility factor obtained from the digital soil attributes mapping

The summary statistics of soil property in Table 4 show soil attributes physical and organic matter variability at 0 to 0.30 m depth (Table 2.4). The low amount of clay and SOM content and high sand content ranging from 73% to 92 % demonstrate soil erosion-prone features and low natural fertility in the soil.

Table 2.4 – Soil attributes values obtained by laboratory analyses.

	Minimum	Maximum	Mean	SD ¹	CV ²
Sand (%)	73.00	92.10	83.27	4.11	16.87
Coarse Sand (%)	42.00	72.70	58.65	7.48	56.01
Fine Sand (%)	13.10	40.50	24.54	5.33	28.38
Silt (%)	1.20	3.80	2.07	0.56	0.32
Clay (%)	6.70	23.20	14.74	3.64	13.25
SOM ³ (%)	0.70	2.10	1.19	0.19	0.04

¹ Standard deviation; ² Coefficient of variation; ³ Soil organic matter.

The geology map (PERROTTA et al., 2005) showed that sandy-mudstone lithology of the Rio do Peixe Valley's formation is predominant along with the site where the relief is flat featuring Ferralsol (LV, LA, LVA) to gently undulating characterizing Lixisol (PV, PA, PVA) (Fig 2.5 and Table 2.5)(BERTONI, J., LOMBARDI NETO F., 2017). By approaching the rolling uplands, the sandstone from the Marilia formation arises. Basic intrusive diabase rocks occur between the sand-mudstone of the Serra Geral formation neighboring the site, which

provides the reddish color to the soil types and clay accumulation in the Lixisol subsurface (Fig 2.5). Ferralsols, Lixisol, and Gleysols represent 40%, 58%, and 2% of the land, respectively.

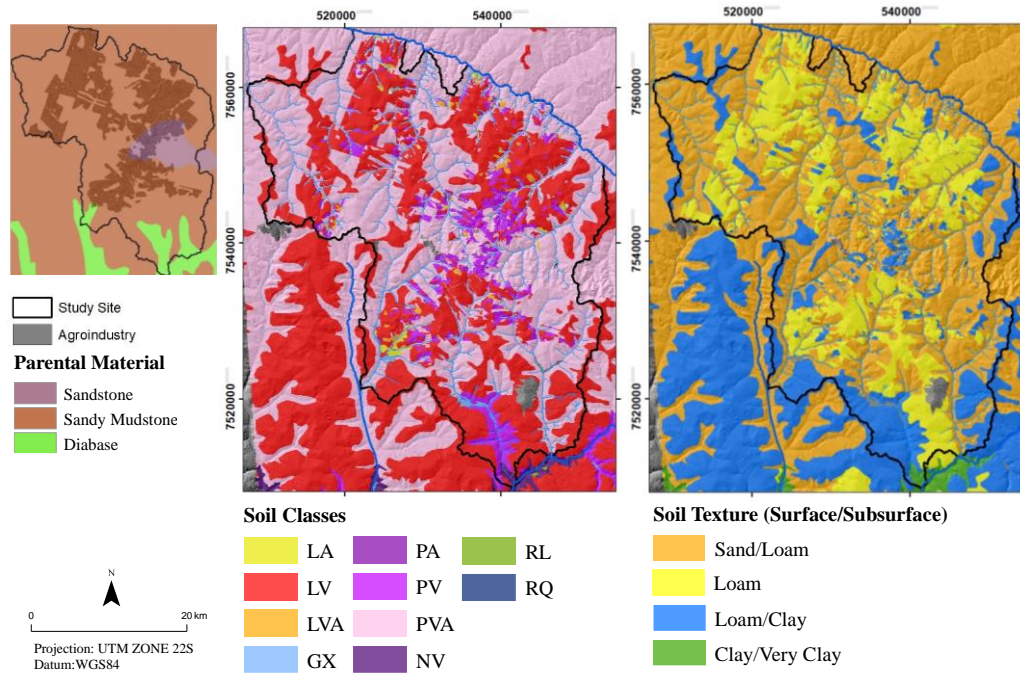


Figure 2.5. Maps of: a) Lithology (MEZZALIRA, 1966), b) Soil classes, c) Topsoil class texture.

Soil permeability were established based on soil type, color and texture (Fig. 2.5 and Table 2.5). Permeability decreases as color change from reddish to yellowish and from sandy to clay texture. We classified the soil classes, in dry conditions, from the agroindustry map and the regional map (ROSSI, 2017) at the suborder level according to the Brazilian Soil Classification System (SiBCS) (DOS SANTOS et al., 2018) and the corresponding classes of the World Reference Base (FAO, 2014).

The multi-temporal satellite bare soil resulted in 35 years of Landsat data from 1984 to 2019 (Fig. 2.6 a). The synthesis of all images composes a final image of bare soil, covering 72% of the cropland surface (Fig. 2.6 b). The soil surface corresponds to the agricultural inventory data, in which there is a specific time-window to monitor soil surface satellite imaging due to the conventional crop management tillage adopted. The remaining sites correspond to forest or grass assigned as NA values for modeling.

Table 2.5 – Permeability according to soil class type, color and texture.

SiBCS¹	WRB²	Color	Texture	Permeability³
Gleissolo Háplico (GX)	Gleysol			Very Slow
Latossolo Amarelo (LA)	Ferralsol	Yellow	Loam	Moderate
Latossolo Vermelho (LV)	Ferralsol	Red	Loam	Moderate to Fast
Latossolo Vermelho (LV)	Ferralsol	Red	Clay	Moderate
Latossolo Vermelho-Amarelo (LVA)	Ferralsol	Red - Yellow	Loam	Moderate to Fast
Latossolo Vermelho-Amarelo (LVA)	Ferralsol	Red - Yellow	Clay	Moderate
Nitossolo Vermelho (NV)	Nitisol	Red	Clay	Moderate to Fast
Argissolo Amarelo (PA)	Lixisol	Yellow	Sand/Loam	Slow to Moderate
Argissolo Amarelo (PA)	Lixisol	Yellow	Loam /Clay	Slow
Argissolo Vermelho (PV)	Lixisol	Red	Sand/Loam	Slow to Moderate
Argissolo Vermelho (PV)	Lixisol	Red	Loam/Clay	Slow
Argissolo Vermelho-Amarelo (PVA)	Lixisol	Red - Yellow	Sand/Loam	Slow to Moderate
Argissolo Vermelho-Amarelo (PVA)	Lixisol	Red - Yellow	Loam/Clay	Slow
Neossolo Litólico (RL)	Leptsol		Clay	Slow
Neossolo Quartzarênico (RQ)	Arenosol		Sand/Loam	Fast

¹ Brazilian Soil Classification System (DOS SANTOS et al., 2018). ² World Reference Base (IUSS, 2015).

The spatial-spectral patterns are related to the soil mineralogy, granulometry and organic matter content identified throughout the satellite image's color and the spectral data (Fig. 2.6 c). Bright colors indicate low soil organic carbon content and higher quartz proportions (DEMATTE et al., 2020). The shape and intensity of spectral profile discriminate sandy soil as it increases from the higher reflectance and the ascending shape of the wavelength from Band 1 to Band 5 (GALLO et al., 2018).

The spectral signatures of the surface reflectance provided from the site-specific soil samples validate the bare soil composite image's reliability and quality. While, the validation prediction of clay, fine sand, silt, and organic matter maps correspond to R^2 of 0.67, 0.59, 0.68 and 0.55 and RMSE (g kg^{-1}) of 25.8, 48.3, 4.38, 1.99 respectively, which indicate good agreement and low error between the observed and the predicted dataset.

The spatial distribution of K-Factor values increases where PVA and PV occur in rolling uplands, as observed in sub-basin 10 (Fig. 2.7). In these sites, the sand-loamy textures soil

particles are easily detached and transported by overland flow. The mean K-Factor value for the agricultural study site corresponds to $0.019 \text{ tons h MJ}^{-1} \text{ mm}^{-1}$. Predicted versus measures K-Factor values present satisfactory performance with an R^2 of ~ 0.78 (Fig. 2.8).

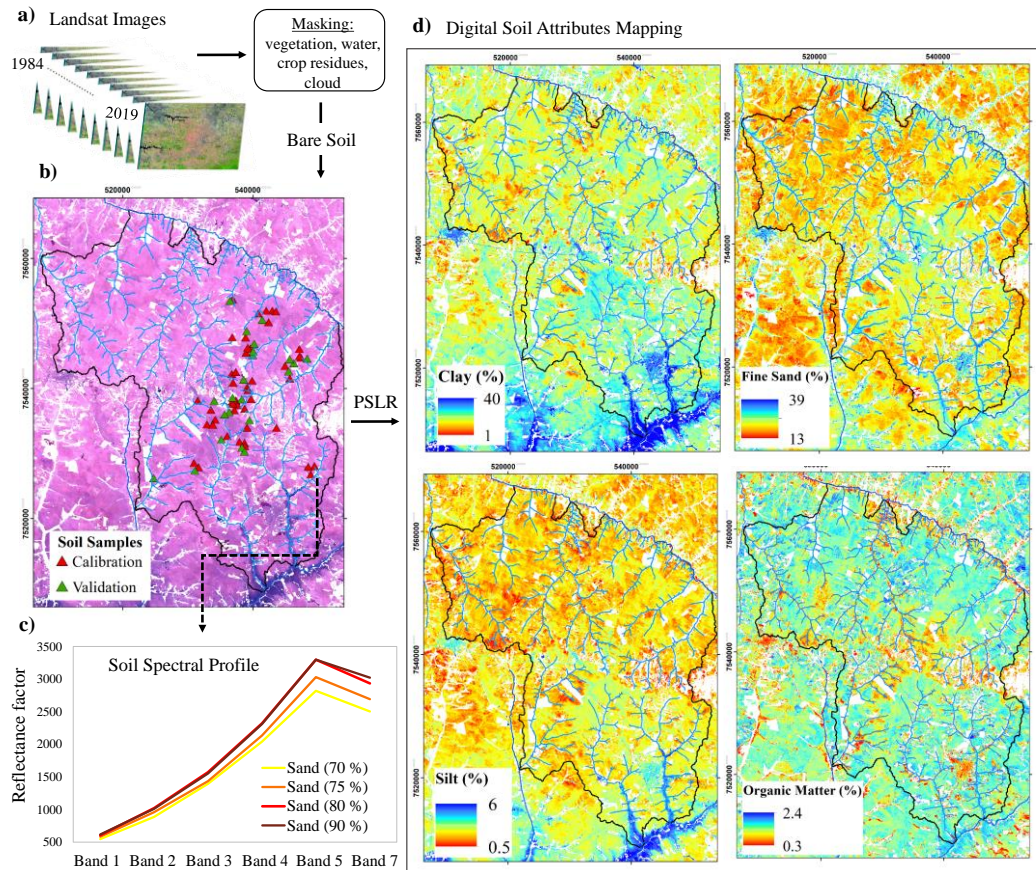


Figure 2.6. a) Multi-temporal satellite images masks using NDVI e MID-Infrared, b) Soil Synthetic Imagen has shown the agricultural land in false color (RGB 543) of the Landsat data with soil samples sites location used for the soil map attributes prediction by Partial Square Least Regression, c) Soil spectral profile average from the soil samples, d) Soil attributes map (clay, fine sand, silt, and organic matter) used to derive the erodibility factor map. Soil texture analyzes resulted in the following classes: Sand, Coarse Sand, Fine Sand, Silt and Clay. Note that only Clay, Fine Sand and Silt maps were generated to calculate erodibility, so the final percentage value will not be 100%. This would require all maps of all textural classes to reach 100%.

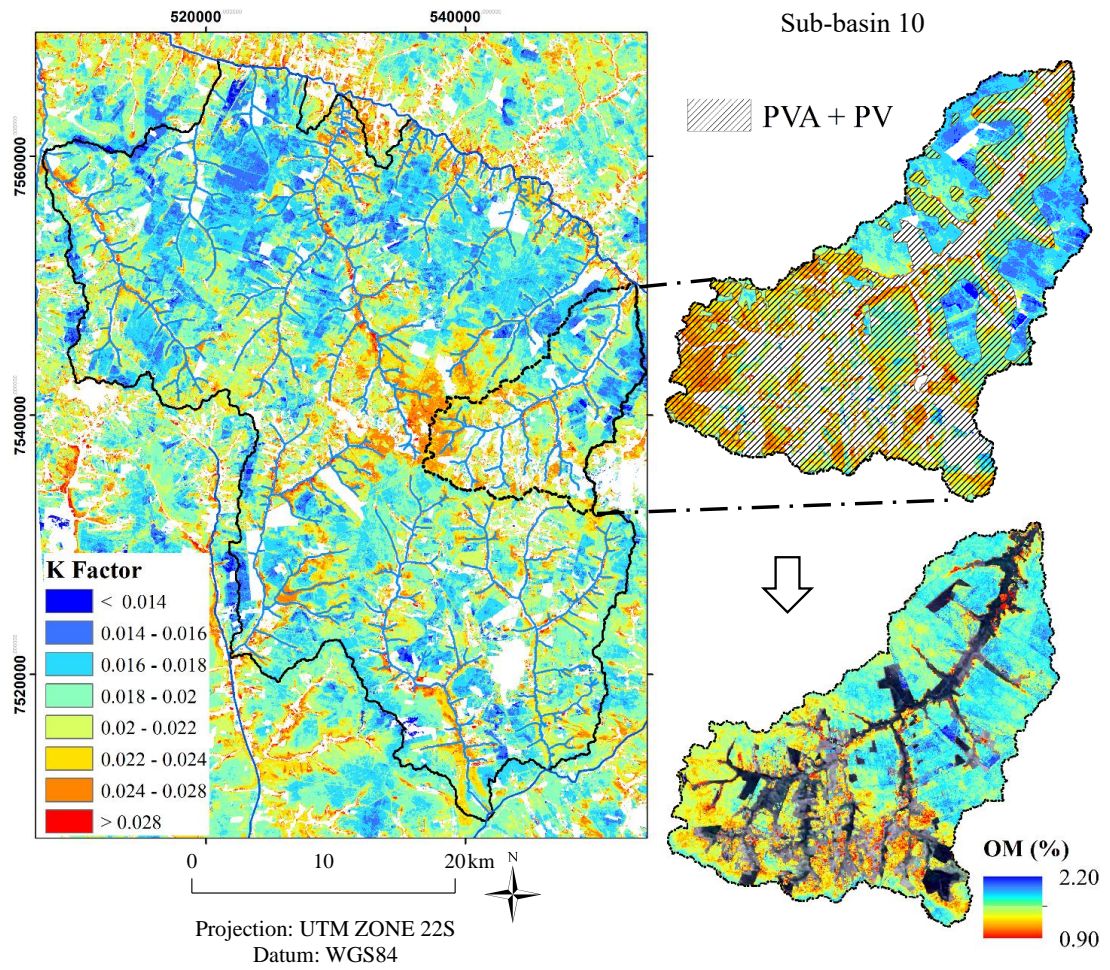


Figure 2.7. Soil K-Factor derived from satellite base-estimation contrasting organic matter values at sub-basin 10.

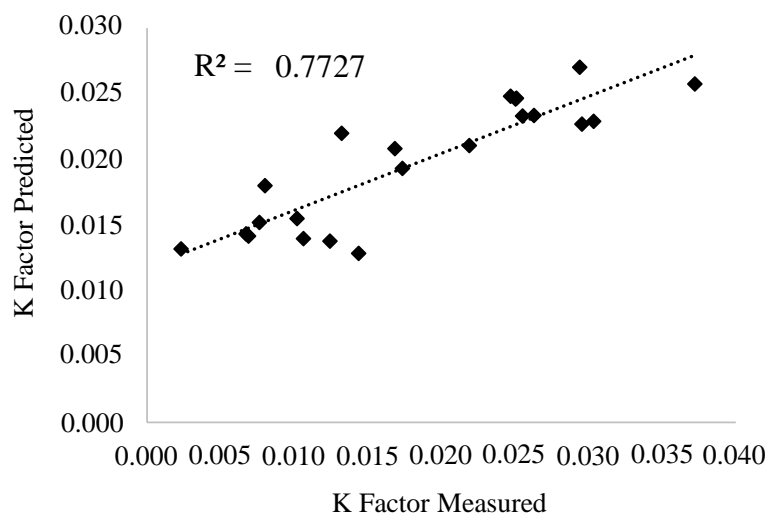


Figure 2.8. Comparison between the K-Factor satellite-based predicted and K-Factor measured by the soil samples analysis.

2.3.1.3 The topographic parameters and control practice

LS-Factor derived from flow accumulation, flow direction, and slope using Digital Elevation Model (DEM) performed at GIS incorporates surface runoff into soil erosion (Fig. 2.9). The L-Factor stretches the impact of slope length while the S-Factor delivers the effect of slope steepness. The DEM captured the topography changes with precision and estimated soil erosion with accuracy. (DESMET; GOVERS, 1996) demonstrated that the LS-Factor model is suitable for landscape-scale soil erosion modeling.

The LS-Factor's topographic spatial pattern presents an average value of 0.58, with a range of 0.03 in lowland to 82 in the uplands (Fig. 8). The coefficient of variation (CV) of 0.53 indicates low heterogeneity; LS-Factor value under 1.5 was estimated in 93% of the area.

P-Factor map depended on slope derived from DEM and contouring as specific support management (Fig. 2.8). The P-Factor result presents low variation; 88% of the area has represented a value from 0.5 to 0.6 with an average of 0.59.

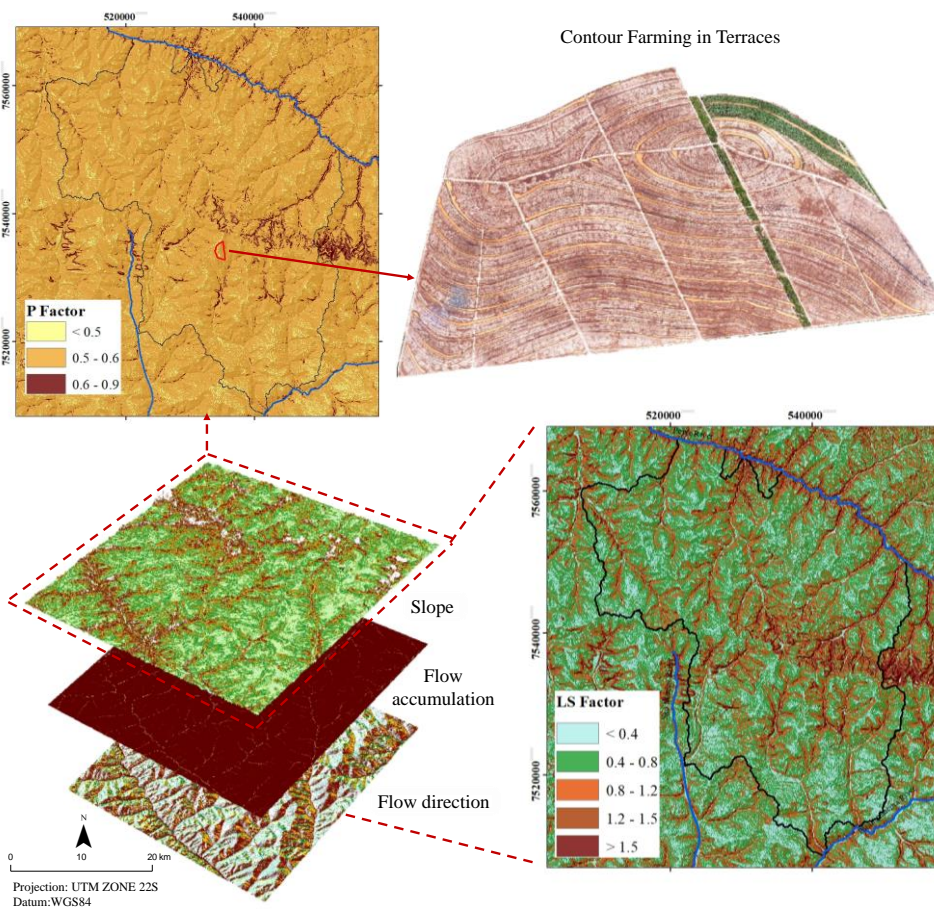


Figure 2.9. LS-Factor derived from the SRTM variables (slope, flow accumulation and flow direction) and P-Factor derived from slope and contour farming a support conservation practice.

2.3.1.4 Cover management factor

The spatial C-Factor of crop residue management for the scenarios expresses the land use management applied from 2013 to 2017 (Fig. 2.10). It generated 98 combinations of sugarcane management in the cropland plots. We can observe in sub-basin 7 the cropland plots contrasting two tillage combinations. The sugarcane cycles range from one to nine in the unit plots; the mean is five crop cycles (Fig. 2.11). During the sugarcane crop cycle, plant cane had higher production and the yield decay over the next years (Fig. 2.11 b). We can observe that about 80% of the area is productive during the year, while the remaining area is under replanting (Fig. 2.11 a).

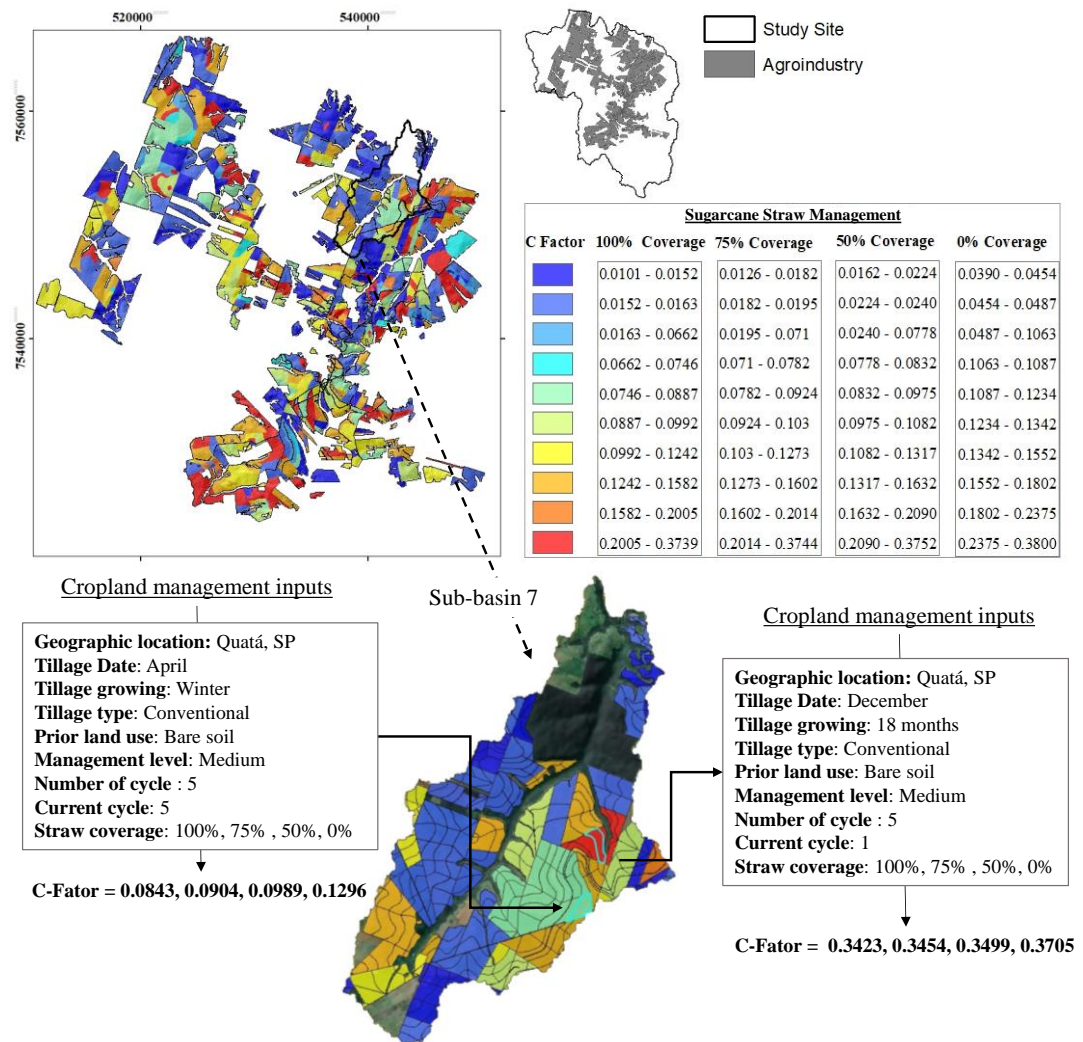


Figure 2.10. C-Factor of the agroindustry under 100 % coverage sugarcane straw coverage, 50% coverage, 75% coverage, and no coverage, and the sub-basin 7 representing two cover management input data in each arable cropland plot.

During the sugarcane replanting period, the crop residues are incorporated into the soil by tillage operations, and the soil is exposed, characterizing the prior land use subfactor as bare soil for all the cropland plots. The average C-Factor values from the cropland plots for 0%, 50%, 75%, and 100% coverage are 0.12, 0.0975, 0.0921 and 0.0884, respectively. We applied this C-Factor value for the entire sub-basins dimension.

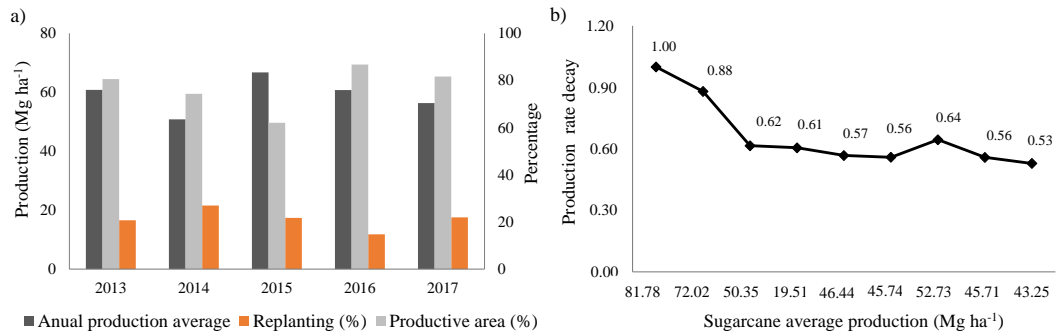


Figure 2.11. a) Yield production areas from 2013 to 2017 with an average annual production considering all sugarcane cycles and the replanting areas. b) The average yield in nine sugarcane crop cycle with production rate decay.

2.3.2 Soil loss in agricultural regions

The soil loss rates from high-resolution spatially distributed modeling (30 x 30 m cell size) were estimated by integrating the erosivity, erodibility, topography, conservative practices, and cover management data. Our results showed that soil erosion dynamics under different straw coverage rates (Fig. 2.12) decreases soil loss rates by 22 %, 26 % and 28 % in all sub-basins as the amount of straw coverage increases from to 50 %, 75 % to 100%, respectively (Table 2.6).

The average bulk density of 1.69 Mg m⁻³ derived soil loss tolerance (T-value); T-value presents an area-specific average of 4.3 Mg ha⁻¹. Our data demonstrate that the annual average soil erosion exceeds the T-value threshold in 12 of the 13 sub-basins under no cover of straw (Table 6). Sub-basin 3, 6, 7 show soil loss per percentage of the land lower than the T-value (Fig 2.12 a).

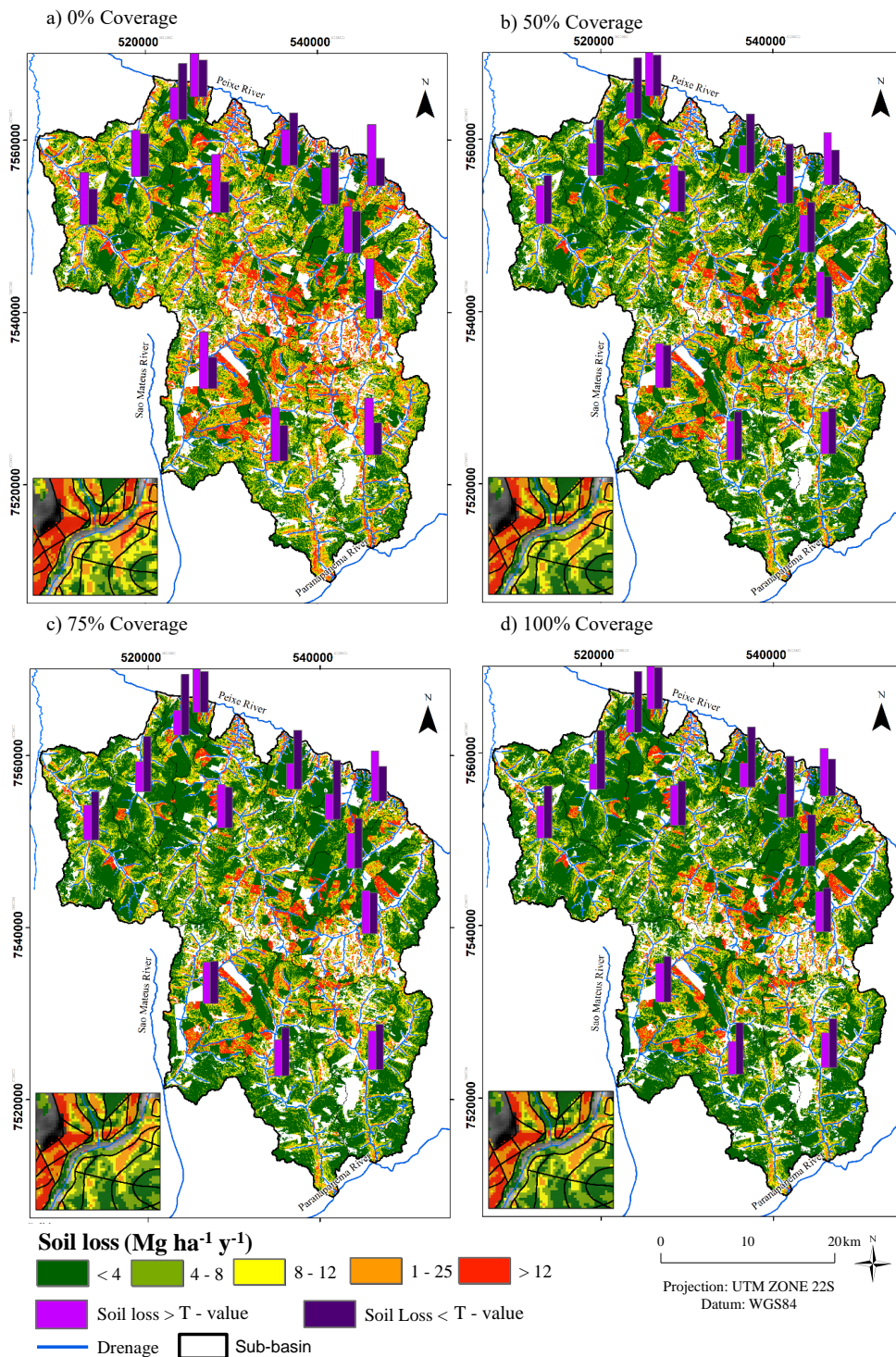


Figure 2.12. Soil loss obtained by the RUSLE model and the percentage of the basin with greater and lesser soil loss than the tolerance (T-value) with a) 0% straw coverage rate, b) 50% straw coverage, c) with 75% straw coverage, d) 100% straw coverage.

The most intensively eroded region were identified in sub-basins 4, 8, 9, 10, 11, 13 with an annual average soil erosion higher than T-values in sites 100% covered with straw (Table 2.6). Sub-basin 4 presented the lowest values of total soil loss (52.65 Mg x 103yr⁻¹) (Table

2.4), due to the smaller size of the sub-basin compared to the others. The average soil loss scenario of 100 % straw coverage is equivalent to T-value (Table 2.6), indicating that all the amount of straw is necessary to balance soil loss tolerance from the perspective of soil erosion. Thus, it is equivalent to 7 Mg⁻¹ of straw according to the sugarcane yield data documented (Fig 2.11). However, this amount of straw has not been satisfactory to protect the soil against erosion in 40% of the agricultural land, classified with a higher potential of soil erosion estimated at ~ 6,000 Mg 103 y⁻¹ (Fig 2.12a, Table 2.6). We estimated an overall increase in soil erosion amount of 4 %, 10 %, and 41 % under 75%, 50% and no coverage, respectively, driven by the possibility of spatial removal.

Table 2.6 - Average soil erosion and total soil loss per sub-basin

Sub-basin	Average soil erosion (Mg ha ⁻¹ yr ⁻¹)				Total soil loss (Mg x 10 ³ yr ⁻¹)			
	0%	50%	75%	100%	0%	50%	75%	100%
1	5.74	4.35	4.10	3.93	832.09	631.024	494.67	569.71
2	4.83	3.73	3.59	3.39	432.27	333.741	321.65	303.37
3	4.19	3.31	3.14	3.02	125.86	99.25	94.10	90.48
4	7.53	6.39	6.18	6.04	65.65	55.69	53.90	52.65
5	6.11	4.82	4.58	4.41	1,645.55	1,297.30	1,232.67	1,188.52
6	4.59	3.33	3.09	2.93	269.72	195.55	181.72	172.24
7	4.89	3.75	3.52	3.35	206.67	158.49	148.60	141.68
8	7.30	5.70	5.38	5.16	103.54	80.87	76.35	73.28
9	6.52	5.10	4.79	4.57	535.56	419.43	393.70	375.45
10	7.62	5.84	5.50	5.26	942.35	722.981	680.03	650.71
11	6.97	5.64	5.37	5.18	1,093.39	883.75	841.35	811.81
12	5.86	4.59	4.35	4.18	1,050.64	822.95	780.04	750.33
13	6.38	4.92	4.65	4.46	1,102.66	850.13	803.35	771.01
Total area	6.04	4.73	4.48	4.30	8,406.01	6,551.20	6,202.47	5,951.31

2.4 DISCUSSION

The soil is vulnerable for erosion by nature through according to a slow constructive process of fertile soils caused by geology, topography and climate factors. In contrast, anthropogenic land-use changes and unsustainable land management in agriculture can accelerate land degradation (LAL, 2003).

In this paper we assessed a multi-temporal soil erosion pattern driven by water in sugarcane fields using the RUSLE model at 30 m resolution. We used remote sensing data and GIS techniques to extract R, K, LS factors and, an exhaustive set of C-Factor, an accurate DEM to compute LS and P factors, and an innovative digital soil mapping method to calculate K-Factor. Thus, the variability demonstrated by this method has a considerable potential to identify hotspots and concern areas for both uses in the cropland plots scale and the whole area for conservation planning (Fig 2.12).

Rainfall intensity emphasizes the region's climatic vulnerability, resulting in high values of erosivity factor (Fig. 2.3 and 2.4), a critical climatic driver of soil erosion. According to (VRIELING; HOEDJES; VAN DER VELDE, 2014), erosivity correlates with total rainstorm energy to the storm's maximum 30 minutes of rainfall intensity. The spatial variability of erosion power of rainfall tends to increase or decrease in various combinations driven to the degree of global warming caused by climate change (OLIVER, 1980), which impact directly on land degradation, resulting in increasing temperatures, changing rainfall patterns, and intensification of rainfall (OLSSON et al., 2019).

Individual powerful rainstorms of a short period can remove topsoil during a rainstorm event, initiate a gully and mudslide, as revealed in Fig 2.1. Damages caused by heavy rainfall events have a century-scale nutrient depletion, soil particle loss, and high-water treatment costs. The 3-hourly TRMM data provided a good indicator of high-intensity rainfall events (more than 30 mm), typically captured at the beginning of the rainy season (VRIELING et al., 2008).

Hydrological changes affect soil fertility due to topsoil layer removal, water availability, and the vulnerability of smallholder and subsistence agriculture (MORTON, 2007). Each soil type has properties that have different resistance to the raindrop and runoff. High rainfall erosivity increases soil loss rates that deplete soil structure (breakdown aggregates) and accelerate the decomposition of the organic carbon matter by a microbial process (LAL, 2003). Controversially, a decrease in rainfall erosivity may enforce agribusiness development (ALMAGRO et al., 2017) and smallholders, especially in regions with crop irrigation liability. While, a decrease of rainfall erosivity in the Southeast region of Brazil may suggest a favorable scenario for the continued sugarcane expansion (ALMAGRO et al., 2017) since sugarcane does not need irrigation (GOLDEMBERG et al., 2014).

Projection of climate change in rainfall erosivity is essential, but at this stage, developing strategies to adapt to these changes is the key to reduce vulnerabilities and improve resilience, e. g., public policies that focus on soil and water conservation, such as sustainable agriculture and conservation practices must be encouraged, ensuring food security and energy.

Our digital soil attributes maps obtained extracted from satellite data are instruments for sustainable land-use (Fig. 2.6). Previous studies based on Landsat data have also derived reliable soil proprieties maps demonstrating the substantial potential of these products for the land management applications (DIEK et al., 2017; DOGAN; KILIÇ, 2013; MENDES et al., 2019; SHABOU et al., 2015). We identified that sites with moderate soil loss are mostly homogeneous with topsoil texture that varies from loam to sandy. The loam texture sites demonstrate the occurrence of Ferralsols (Fig. 2.5) in the flat position of the landscape. On the other hand, high soil loss occurs mostly in Lixisol (Fig. 2.5) that is over smooth to gently undulating relief with the textural gradient of sandy/loamy at the surface and loamy/clayey in subsurface layers (Fig. 6), featuring the highest values of LS-Factor (Fig. 2.9). We confirmed (MANNIGEL et al., 2002) assumption that an increase of the textural gradient leads to a decrease in soil loss tolerance and an increase in soil K-Factor (Fig. 2.7).

SYSI data can capture the agricultural land-use change. Here, we could enlighten two time periods to investigate land-use change using SYSI 1) From 1984 to 2009, the period with land changes from forestation to sugarcane under harvest burning system adoption; 2) after 2009, with the establishment of the current machine harvest system characterized by the remarkable effect of soil conservation agriculture provided by straw on topsoil. On the other hand, straw removal practices may threaten sugarcane yield, compromising bioenergy production (CARVALHO et al., 2019). The nutrient addition in soil in the first period, associated with straw removal of the second period plus the climate change impacts related to land use cover may be re-sponsible for soil organic matter depletion (CARVALHO et al., 2019; TENELLI et al., 2019b). Our investigations reveal that high erodibility values in sub-basin 10 correspond to Lixisols, associated with the low organic matter content (Fig. 2.7). Lixisols when exposed due to changes in land use and/or soil management, erosion processes are favored. These soils have a more clayey B horizon, which reduces water infiltration, favoring surface runoff and, consequently, erosion.

Strategies for soil conservation as cover management are the main component to control soil erosion potential of runoff, maintain soil structure and conserve soil organic carbon with low cost (PANAGOS et al., 2015). Crop residue retained in the field delivers maintenance to the soil quality; it affects sugarcane yields in all soil types in different magnitudes. Straw can help maintaining soil moisture and, mitigating water deficit, which stimulates microclimate by regulating the thermal amplitude and improving the soil biota (CARVALHO et al., 2017; RUIZ CORRÊA et al., 2019). The yield annual average, inferior to the national average yield of 76 Mg ha⁻¹ (CONAB, 2020) (Fig 2.11a) aggregated with soil compaction, reveals low soil fertility.

Field observations and the literature indicated high soil compaction in this region, particularly if straw has been removed (CASTIONI et al., 2019), which resulted in low soil permeability capacity.

Ferralsol is very well-developed, deep and unsaturated, characterized as fast permeability. However, this soil was classified as moderate to fast or moderate. We also observed that permeability decreases as color changes from reddish to yellowish and sandy to clay texture (Table 5). Whereas, as permeability decreases more vulnerable is topsoil loss in Lixisol that is well-developed with a textural gradient in the subsurface featuring erosion-prone soils (MEDEIROS et al., 2016). These attributes result in low yielding potential and straw production. It explains the inefficiency of 100% straw coverage capacity of holding gross erosion and preventing soil degradation in many sub-basins, especially in sub-basin 4 and 8 that presented the soil erosion hotspots (Fig 2.12d and Table 2.6), even under a low heterogeneity topography (Fig. 2.9).

Our C-Factor results demonstrate that the number of sugarcane cycle and the planting season are the SLR sub-factors that have the most significant impact on the management cover, consistent with (ROCHA, 2017). The sugarcane cycle can influence crop residue maintenance in the erosion process by surface-cover, canopy-cover, and tillage effectiveness in the yielding. While the planting season is affected by the climate, the soil is affected by the following conditions: *i*) During replanting when the soil is entirely uncovered; *ii*) At the beginning of the sugarcane ratoon, the previous cycle removed the straw, and the sugarcane canopy-cover is not entirely close; *iii*) The low number of sugarcane cycles (less than five due to the low yield and coverage potential; *iv*) Tillage management operations during the rainy season.

Alternative management strategies on-site for more sustainable sugarcane production is required to compensate the adverse erosion effects on soil, water, and biotic balance as vegetative barrier conservation practices (BONNER et al., 2014), and techniques to improve soil organic carbon and increase yield e. g., reduce or no-tillage, crop rotation (minimum soil disturbance) (TENELLI et al., 2019b) legume cover crop (TENELLI et al., 2019a), organic fertilizer, filter cake, ashes, biochar, and other. Reduce tillage, and no-tillage system concepts were implemented in this century. Reduced tillage system associated with a part of the straw cover in the soil could enhance soil organic carbon stock, sustain sugarcane yield over the crop cycle, and part of the straw used for bioenergy (TENELLI et al., 2019b). Each agricultural system affects short-term soil CO₂ emissions. Undisturbed soil keeps high soil moisture than conventional tillage; moisture is a control temporal variability factor of CO₂ emission. The

adoption of no-tillage in sugarcane areas would prevent 30% of soil CO₂ emission in tropical soils than conventional tillage.

The erosion cost could be reduced by 81.2% adopting no-tillage, while the production costs increased only by 0.47 for the soybean crop (RODRIGUES, 2005). Another study observed the same crop an erosion cost reduction from the different management systems, including no-tillage, reduced tillage and conventional tillage in \$ 15, 16, and 25 ha⁻¹ yr⁻¹, respectively (BERTOL et al., 2007). Soil erosion assessment is essential from an economic perspective since it degrades soils on-site, producing loss of fertility and reduces water storage capacity compromising yield, which from the long-term may depreciate land value (TELLES et al., 2013; TELLES; GUIMARÃES; DECHEN, 2011). The hydrographic basins unit is vital to assess the cost of soil loss due to the off-site impacts of land degradation. Soil erosion effects in the surrounding areas can be severe to the freshwater systems causing sedimentation, eutrophication, enhancing urban areas flooding, and impacting the marine ecosystem.

The results reported herein indicate the conservation-effective measures on-site erosion is essential to reduce or reverse soil degradation, and minimized the climate change impacts from off-site erosion. Furthermore, the obligation of soil conservation practices may help to internalize the costs of the land user. Fertile soil is a limited and non-renewable natural resource, and soil degrades impacts the world from many aspects, e.g., socio-economic, social, political, and cultural for this and future generations.

2.5 CONCLUSION

The method to estimate soil loss indicated soil degradation prone areas that request sustainable land management. The bare soil surface image obtained from multi-temporal satellite images covering 100% of the agricultural land use is equivalent to 72% of the study site. The image's spectral patterns presented accurate spectral quality that permits capturing the soil interactions, featuring sandy soil and low organic matter content properties. Our spatiotemporal erodibility factor reveals the correlation of soil organic matter depletion with high erodibility values in Lixisol, which resulted in low soil loss tolerance.

The bare soil surface technique indicates that intensive farming causes high soil exposure rates in the last three decades. Erosion intensification contributes to land degradation for at least 20 years from the beginning of the multi-temporal series until 2010, when bare soil frequency decreased due to the gradual change to agricultural conservation systems established in the sugarcane fields. Our result indicates vulnerable areas to hold gross erosion in locations with 100 % of crop residue coverage. This susceptible area is a combination of natural erosion-

prone areas with low effectiveness of the tillage practices and the number of cycles (inferior to five) that result in low sugarcane straw yield, which is easily and quickly decomposed by the microbial process. In addition, we suggest further studies using SYSI to deepen soil erosion researches.

Furthermore, the strong rainfall erosivity of the region reinforces soil erosion by water, especially in the planting season. Public policies that focus on soil and water conservation to ensure food and energy security are strategies to reduce the vulnerabilities and improve the resilience of the environment to adapt to the increasing temperatures, the changing of the rainfall patterns, and the rainfall intensification driven by climate change. This technique provides multidisciplinary uses that extend beyond sustainable agriculture developments and land-use change monitoring as the costs to replace nutrients loss derived from soil erosion and carbon stock dynamics are the foundation for the emission levels analyses.

The high-resolution spatially distribution method provided can identify soil degradation prone areas and the cropland expansion frequency. This information may guide farms and the policymakers for a better request of conservation practices according to site-specific management variation.

2.6 REFERENCES

- ALMAGRO, A. et al. Projected climate change impacts in rainfall erosivity over Brazil. **Scientific Reports**, v. 7, n. 1, p. 8130, dez. 2017.
- AMUNDSON, R.; GUO, Y.; GONG, P. Soil diversity and land use in the United States. **Ecosystems**, v. 6, n. 5, p. 470–482, ago. 2003.
- BANWART, S. Save our soil. **Nature**, v. 474, p. 151–152, 2011.
- BENAVIDEZ, R. et al. A review of the (Revised) Universal Soil Loss Equation ((R)USLE): With a view to increasing its global applicability and improving soil loss estimates. **Hydrology and Earth System Sciences**, v. 22, n. 11, p. 6059–6086, 2018.
- BERTOL, I. et al. Aspectos financeiros relacionados às perdas de nutrientes por erosão hídrica em diferentes sistemas de manejo do solo. **Revista Brasileira de Ciência do Solo**, v. 31, n. 1, p. 133–142, fev. 2007.
- BERTONI, J., LOMBARDI NETO F. **Conservação do Solo**. 10th. ed. [s.l: s.n.].
- BONNER, I. J. et al. Modeled Impacts of Cover Crops and Vegetative Barriers on Corn Stover Availability and Soil Quality. **Bioenergy Research**, v. 7, n. 2, p. 576–589, 2014.
- BORDONAL, R. DE O. et al. Sustainability of sugarcane production in Brazil. A review. **Agronomy for Sustainable Development**, v. 38, n. 2, p. 13, 27 abr. 2018a.

BORDONAL, R. DE O. et al. Sugarcane yield and soil carbon response to straw removal in south-central Brazil. **Geoderma**, v. 328, n. May, p. 79–90, out. 2018b.

BORRELLI, P. et al. An assessment of the global impact of 21st century land use change on soil erosion. **Nature Communications**, v. 8, n. 1, 2017.

BORRELLI, P. et al. A step towards a holistic assessment of soil degradation in Europe: Coupling on-site erosion with sediment transfer and carbon fluxes. **Environmental Research**, v. 161, n. May 2017, p. 291–298, fev. 2018.

BRADY, N. C.; WEIL, R. R. **The Nature and Properties of Soils**. 14. ed. New Jersey: Pearson, 2008.

CARVALHO, J. L. N. et al. Input of sugarcane post-harvest residues into the soil. **Scientia Agricola**, v. 70, n. 5, p. 336–344, 2013.

CARVALHO, J. L. N. et al. Agronomic and environmental implications of sugarcane straw removal : a major review. **Bioenergy Research**, p. 1–16, 2016a.

CARVALHO, J. L. N. et al. Agronomic and environmental implications of sugarcane straw removal : a major review. **Bioenergy Research**, p. 1–16, 2016b.

CARVALHO, J. L. N. et al. Contribution of above- and belowground bioenergy crop residues to soil carbon. **GCB Bioenergy**, v. 9, n. 8, p. 1333–1343, ago. 2017.

CARVALHO, J. L. N. et al. Multilocation Straw Removal Effects on Sugarcane Yield in South-Central Brazil. **Bioenergy Research**, v. 12, n. 4, p. 813–829, 2019.

CASTIONI, G. A. F. et al. Straw Removal Affects Soil Physical Quality and Sugarcane Yield in Brazil. **BioEnergy Research**, jul. 2019.

CERVI, W. R. et al. Mapping the environmental and techno-economic potential of biojet fuel production from biomass residues in Brazil. **Biofuels, Bioproducts and Biorefining**, p. 1–23, 2020.

CHAPPELL, A. et al. Minimising soil organic carbon erosion by wind is critical for land degradation neutrality. **Environmental science & policy**, v. 93, p. 43–52, 2019.

CHERUBIN, M. R. et al. Crop residue harvest for bioenergy production and its implications on soil functioning and plant growth: A review. **Scientia Agricola**, v. 75, n. 3, p. 255–272, maio 2018.

CHERUBIN, M. R. et al. Sugarcane Straw Removal: Implications to Soil Fertility and Fertilizer Demand in Brazil. **BioEnergy Research**, ago. 2019.

COLODRO, G. et al. Rainfall erosivity: its distribution and relationship with the nonrecording rain gauge precipitation at Teodoro Sampaio, São Paulo, Brazil. **Revista Brasileira de Ciência do Solo**, v. 26, n. 1, p. 809–818, 2002.

CONAB. Follow-up of the Brazilian harvest: Sugarcane. **Companhia National de Abastecimento**, v. 7, n. Harvest 2020/2021, p. 1–62, 2020.

DE OR MEDEIROS, G. et al. Estimates of annual soil loss rates in the state of São Paulo, Brazil. **Rev. Bras. Ciência Do Solo.**, v. 40, p. 1–18, 2016.

DEMATTE, J. A. M. et al. Geospatial Soil Sensing System (GEOS3): A powerful data mining procedure to retrieve soil spectral reflectance from satellite images. **Remote Sensing of Environment**, v. 212, n. August 2017, p. 161–175, 2018.

DEMATTE, J. A. M. et al. Bare earth's Surface Spectra as a proxy for Soil Resource Monitoring. **Scientific reports**, v. 10, n. 1, p. 1–11, 2020.

DESMET, P. J. J.; GOVERS, G. A GIS procedure for automatically calculating the USLE LS factor on topographically complex landscape units. **Journal of Soil and Water Conservation**, v. 51, n. 5, p. 427–433, 1996.

DIEK, S. et al. Bare Pixel Composite for agricultural areas using landsat time series. **Remote Sensing**, v. 9, n. 12, 2017.

DOGAN, H. M.; KILIÇ, O. M. Modelling and mapping some soil surface properties of Central Kelkit Basin in Turkey by using Landsat-7 ETM+ images. **International Journal of Remote Sensing**, v. 34, n. 15, p. 5623–5640, 2013.

DOS SANTOS, H. G. et al. **Sistema brasileiro de classificação de solos**. [s.l.] Brasília, DF: Embrapa, 2018., 2018.

EMBRAPA. **Manual de métodos de análises**. [s.l.: s.n.].

FAO. **World reference base for soil resources 2014. International soil classification system for naming soils and creating legends for soil maps**. [s.l.: s.n.].

FAOUN. Status of the World's Soil Resources. **Food and Agriculture Organization of the United Nations**, 2015.

FOSTER, G. R. et al. Conversion of the universal soil loss equation to SI metric units. **Journal of Soil and Water Conservation**, v. 36, n. 6, p. 355–359, 1981.

FOSTER, G. R.; MEYER, L. D.; ONSTAD, C. A. A runoff erosivity factor and variable slope length exponents for soil loss estimates. **Transactions of the ASAE**, v. 20, n. 4, p. 683–687, 1977.

FRANCO, H. C. J. et al. Assessment of sugarcane trash for agronomic and energy purposes in Brazil. **Scientia Agricola**, v. 70, n. 5, p. 305–312, 2013.

GALLO, B. et al. Multi-Temporal Satellite Images on Topsoil Attribute Quantification and the Relationship with Soil Classes and Geology. **Remote Sensing**, v. 10, n. 10, p. 1571, 1 out. 2018a.

GALLO, B. C. et al. Multi-temporal satellite images on topsoil attribute quantification and the relationship with soil classes and geology. **Remote Sensing**, v. 10, n. 10, 2018b.

GOLDEMBERG, J. et al. Meeting the global demand for biofuels in 2021 through sustainable land use change policy. **Energy Policy**, v. 69, n. 2014, p. 14–18, 2014.

HUFFMAN, G. J. et al. The TRMM Multisatellite Precipitation Analysis (TMPA): Quasi-Global, Multiyear, Combined-Sensor Precipitation Estimates at Fine Scales. **Journal of Hydrometeorology**, v. 8, n. 1, p. 38–55, fev. 2007.

IPBES. The IPBES assessment report on land degradation and restoration. Montanarella, L., Scholes, R., Brainich, A. (eds). Em: **Secretariat of the Intergovernmental Science-Policy Platform on Biodiversity and Ecosystem Services, Bonn, Germany**. [s.l: s.n.]. p. 1–744.

IPCC. **Climate Change and Land - IPCC Special Report on Climate 21 Change, Desertification, Land Degradation, Sustainable Land Management, Food Security, and Greenhouse gas fluxes in Terrestrial Ecosystems**. [s.l: s.n.].

IUSS. World reference base for soil resources 2014 Update 2015. International soil classification system for naming soils and creating legends for soil maps. Food and Agriculture Organization, Rome. **World Soil Resources Reports**, v. 106, p. 1–203, ago. 2015.

IUSS WORKING GROUP WRB. **World reference base for soil resources 2014. International soil classification system for naming soils and creating legends for soil maps**. [s.l: s.n.].

JONES, C. D. et al. The greenhouse gas intensity and potential biofuel production capacity of maize stover harvest in the US Midwest. **GCB Bioenergy**, v. 9, n. 10, p. 1543–1554, 2017.

LAL, R. **Soil erosion and the global carbon budget**. **Environment International**, jul. 2003.

LOMBARDI NETO, F.; MOLDENHAUER, W. C. Erosividade da chuva: sua distribuicao e relacao com as perdas de solo em Campinas (SP). **Bragantia**, v. 51, n. 2, p. 189–196, 1992.

LORENZ, K.; LAL, R.; EHLERS, K. Soil organic carbon stock as an indicator for monitoring land and soil degradation in relation to United Nations' Sustainable Development Goals. **Land Degradation & Development**, v. 30, n. 7, p. 824–838, abr. 2019a.

LORENZ, K.; LAL, R.; EHLERS, K. Soil organic carbon stock as an indicator for monitoring land and soil degradation in relation to United Nations' Sustainable Development Goals. **Land Degradation & Development**, v. 30, n. 7, p. 824–838, 30 abr. 2019b.

MANNIGEL, A. R. et al. Fator erodibilidade e tolerância de perda dos solos do Estado de São Paulo. **Acta Scientiarum - Agronomy**, v. 24, n. 1990, p. 1335–1340, 2002.

MARTINS-FILHO, M. V. . et al. Soil and Nutrients Losses of an Alfisol with Sugarcane Crop Residue. **Engenharia Agrícola**, v. 29, n. 1, p. 8–18, 2009.

MCCOOL, D. K. et al. Revised Slope Steepness Factor for the Universal Soil Loss Equation. 1987.

MEDEIROS, G. DE O. R. et al. Diagnosis of the Accelerated Soil Erosion in São Paulo State (Brazil) by the Soil Lifetime Index Methodology. **Revista Brasileira de Ciência do Solo**, v. 40, p. 1–15, 2016.

MELLO, C. R. et al. Multivariate models for annual rainfall erosivity in Brazil. **Geoderma**, v. 202–203, p. 88–102, 2013.

MENANDRO, L. M. S. et al. Comprehensive assessment of sugarcane straw: implications for biomass and bioenergy production. **Biofuels, Bioproducts and Biorefining**, v. 11, n. 3, p. 488–504, 2017.

MENANDRO, L. M. S. et al. Soil Macrofauna Responses to Sugarcane Straw Removal for Bioenergy Production. **BioEnergy Research**, v. 12, n. 4, p. 944–957, dez. 2019.

MENDES, W. D. S. et al. Is it possible to map subsurface soil attributes by satellite spectral transfer models? **Geoderma**, v. 343, n. January, p. 269–279, 2019.

MEZZALIRA, S. Instituto Geográfico e Geológico do Estado de São Paulo: Sao Paulo. **Folha Geológica de Piracicaba; Folha SF-23-M-300**, 1966.

MONTGOMERY, D. R. **Dirt: The erosion of civilizations**. [s.l.] Univ of California press, 2012.

MORTON, J. F. The impact of climate change on smallholder and subsistence agriculture. **Proceedings of the National Academy of Sciences of the United States of America**, v. 104, n. 50, p. 19680–19685, 2007.

OLIVEIRA, P. T. S.; WENDLAND, E.; NEARING, M. A. Rainfall erosivity in Brazil: A review. **CATENA**, v. 100, p. 139–147, jan. 2013.

OLIVER, J. E. Monthly precipitation distribution: a comparative index. **The Professional Geographer**, v. 32, n. 3, p. 300–309, 1980.

OLSSON, L. et al. Land degradation: IPCC special report on climate change, desertification, land 5 degradation, sustainable land management, food security, and 6

greenhouse gas fluxes in terrestrial ecosystems. Em: **IPCC Special Report on Climate Change, Desertification, Land 5 Degradation, Sustainable Land Management, Food Security, and 6 Greenhouse Gas Fluxes in Terrestrial Ecosystems**. [s.l.] Intergovernmental Panel on Climate Change (IPCC), 2019. p. 1.

OSTOVARI, Y. et al. Soil loss prediction by an integrated system using RUSLE, GIS and remote sensing in semi-arid region. **Geoderma Regional**, v. 11, n. June, p. 28–36, 2017.

PANAGOS, P. et al. Modelling the effect of support practices (P-factor) on the reduction of soil erosion by water at European scale. **Environmental Science and Policy**, v. 51, p. 23–34, 2015.

PANAGOS, P.; BORRELLI, P.; MEUSBURGER, K. A New European Slope Length and Steepness Factor (LS-Factor) for Modeling Soil Erosion by Water. **Geosciences**, v. 5, n. 2, p. 117–126, 2015.

PANAGOS, P.; BORRELLI, P.; ROBINSON, D. FAO calls for actions to reduce global soil erosion. **Mitigation and Adaptation Strategies for Global Change**, v. 25, n. 5, p. 789–790, 2020.

PERROTTA, M. M. et al. **Mapa geológico do estado de São Paulo, escala 1:750.000. Programa levantamentos geológicos básicos do Brasil, CPRM, São Paulo.** , 2005.

RENARD, K. G. et al. **Predicting Soil Erosion by Water: A Guide to Conservation Planning With the Revised Universal Soil Loss Equation (RUSLE)**. U.S. Depar ed. [s.l: s.n.].

ROCHA, G. C. DA. **Conservação do solo e cana-de-açúcar: aspectos legais e bibliométricos e uma ferramenta de determinação do Fator C (RUSLE)**. Universidade de São Paulo, , 2017.

RODRIGUES, W. Valoração econômica dos impactos ambientais de tecnologias de plantio em região de Cerrados. **Revista de Economia e Sociologia Rural**, v. 43, n. 1, p. 135–153, mar. 2005.

ROQUE, C. G.; CARVALHO, M. P.; PRADO, R. M. Fator erosividade da chuva de Piraju (SP): distribuição, probabilidade de ocorrência, período de retorno e correlação com o coeficiente de chuva. **Revista Brasileira de Ciência do Solo**, v. 25, n. 1, p. 147–156, 2001.

ROSSI, M. **Mapa pedológico do Estado de São Paulo: revisado e ampliado**. [s.l: s.n.]. v. 124

RUIZ CORRÊA, S. T. et al. Straw Removal Effects on Soil Water Dynamics, Soil Temperature, and Sugarcane Yield in South-Central Brazil. **BioEnergy Research**, v. 12, n. 4, p. 749–763, dez. 2019.

SAFANELLI, J. L. et al. Multispectral Models from Bare Soil Composites for Mapping Topsoil Properties over Europe. **Remote Sensing**, v. 12, n. 1369, p. 1–22, 2020.

SHABOU, M. et al. Soil clay content mapping using a time series of Landsat TM data in semi-arid lands. **Remote Sensing**, v. 7, n. 5, p. 6059–6078, maio 2015.

SILVA, A. G. B. et al. How Much Sugarcane Straw is Needed for Covering the Soil? **BioEnergy Research**, jul. 2019.

SMITH, R. M.; STAMEY, W. L. Determining the range of tolerable erosion. **Soil Science**, v. 100, n. 6, p. 414–424, 1965.

STEVENS, C. J. et al. The effects of minimal tillage, contour cultivation and in-field vegetative barriers on soil erosion and phosphorus loss. **Soil and Tillage Research**, v. 106, n. 1, p. 145–151, 2009.

TANYAŞ, H.; KOLAT, Ç.; SÜZEN, M. L. A new approach to estimate cover-management factor of RUSLE and validation of RUSLE model in the watershed of Kartalkaya Dam. **Journal of Hydrology**, v. 528, p. 584–598, 2015.

TELLES, T. S. et al. Valuation of soil erosion costs Scientia Agricola. **Sci. Agric.** v, v. 70, n. 3, p. 209–216, 2013.

TELLES, T. S.; GUIMARÃES, M. D. F.; DECHEN, S. C. F. The Costs of soil erosion. **Revista Brasileira de Ciência do Solo**, n. 1, p. 287–298, 2011.

TENELLI, S. et al. Legume nitrogen credits for sugarcane production: implications for soil N availability and ratoon yield. **Nutrient Cycling in Agroecosystems**, v. 113, n. 3, p. 307–322, 2019a.

TENELLI, S. et al. Can reduced tillage sustain sugarcane yield and soil carbon if straw is removed? **BioEnergy Research**, v. 12, n. 4, p. 764–777, dez. 2019b.

TENELLI, S. et al. Can reduced tillage sustain sugarcane yield and soil carbon if straw is removed? **BioEnergy Research**, v. 12, n. 4, p. 764–777, 26 dez. 2019c.

TENG, H. et al. Assimilating satellite imagery and visible-near infrared spectroscopy to model and map soil loss by water erosion in Australia. **Environmental Modelling and Software**, v. 77, p. 156–167, 2016.

U.S. Department of Agriculture, Agricultural Research Service and Soil Conservation Service. Joint Conference on Slope-Practice, Washington, DC, USA., 1956.

VRIELING, A. et al. Timing of erosion and satellite data: A multi-resolution approach to soil erosion risk mapping. **International Journal of Applied Earth Observation and Geoinformation**, v. 10, n. 3, p. 267–281, 2008.

VRIELING, A.; HOEDJES, J. C. B.; VAN DER VELDE, M. Towards large-scale monitoring of soil erosion in Africa: Accounting for the dynamics of rainfall erosivity. **Global and Planetary Change**, v. 115, p. 33–43, abr. 2014.

VRIELING, A.; STERK, G.; DE JONG, S. M. Satellite-based estimation of rainfall erosivity for Africa. **Journal of Hydrology**, v. 395, n. 3–4, p. 235–241, dez. 2010.

WALTER, A. et al. Brazilian sugarcane ethanol: developments so far and challenges for the future. **Advances in Bioenergy: The Sustainability Challenge**, p. 373–394, 2016.

WISCHMEIER, W. H.; SMITH, D. D. Predicting rainfall erosion losses. a guide to conservation planning. 1978.

YANG, X. et al. Hillslope erosion improvement targets: Towards sustainable land management across New South Wales, Australia. **CATENA**, v. 211, p. 105956, 2022.

CHAPTER 3. FINAL CONSIDERATIONS

Using multitemporal satellite imagery in remote sensing has provided valuable insights into soil properties, relief, climatic conditions, and management practices for monitoring cropland fields and identifying areas at risk of soil loss. The information obtained is crucial for promoting sustainable land use in the study region's crop field.

This study found that high sand content is prevalent in the study region, and optimal management of sugarcane straw alone is insufficient to protect soil against erosion. Alternative conservation practices, such as cover cropping, minimum tillage, counter lines, and terracing, should be immediately adopted to increase organic matter content and promote soil health. Furthermore, in regions where sugarcane straw can be used for the bioenergy industry, continued research, innovation, and policy support are necessary to ensure sustainable use for conservation and bioenergy.

Soil conservation is critical to promoting soil diversity, sustainable agriculture, protecting the environment, and ensuring the well-being of future generations. By adopting soil conservation practices and policies, we can restore degraded soils, increase food production, and mitigate the impacts of climate change.

This study contributes to the existing knowledge on soil conservation and highlights the potential of remote sensing techniques in monitoring and mitigating soil degradation in agricultural landscapes. It provides valuable insights for policymakers and farmers to adopt sustainable agriculture practices. Overall, collaborative efforts among stakeholders are necessary to ensure the sustainable use of our land resources.

Model Limitation

While the Revised Universal Soil Loss Equation (RUSLE) has proven to be a valuable tool for assessing soil erosion risk, its application using satellite imagery and remote sensing has limitations. One notable challenge lies in the inherent complexity of the RUSLE model itself. The model's accuracy heavily relies on the availability and accuracy of input data, which includes factors such as rainfall erosivity, soil erodibility, topography, cover and management practices, and conservation support practices. Remote sensing can provide data for some of these factors, such as land cover and topography. However, certain parameters may be challenging to accurately derive solely from satellite imagery as an erodibility factor.

Soil erosion is a spatially and temporally dynamic phenomenon. It varies across different landscapes and over varying time scales, influenced by short-term climatic events and longer-term trends. This dynamic nature complicates the design of experiments, as researchers

need to capture a wide range of conditions to ensure the robustness and generalizability of their findings. Such complexity often requires extensive data collection and monitoring efforts, making experiments resource-intensive and time-consuming.

Our multitemporal satellite imagery in remote sensing has provided valuable insights into soil properties, relief, climatic conditions, and management practices for monitoring cropland fields. However, the model assumes some constant sub factors data to estimate soil erodibility, such as bulk density determination, which might not hold in dynamic landscapes.

Another limitation arises from the scale at which RUSLE operates. While satellite imagery offers a wide coverage area, the model's success is often contingent upon the analysis and data resolution scale. RUSLE assumes uniform conditions within a given grid cell, which might not always accurately reflect the actual heterogeneity of land use and management practices present within that cell. Additionally, the temporal resolution of satellite imagery may not align with the frequency of erosion events, leading to potential inaccuracies in erosion predictions. Moreover, the model does not account for factors such as ephemeral gullies or channel erosion, which can play a significant role in erosion dynamics but are often not captured by remote sensing data.

In summary, while integrating RUSLE with remote sensing holds promises for assessing soil erosion risk, it is important to acknowledge its limitations. These include the challenge of accurately deriving certain input parameters from satellite imagery and the inherent assumptions and scale-related constraints. Therefore, a holistic approach that combines remote sensing data with field measurements and other research modeling techniques must be continued to encourage policy support.

While remote sensing offers the advantage of capturing erosion patterns over large areas, its effectiveness in providing fine-scale details required for robust validation is restricted. Remote sensing data might lack the resolution necessary to account for localized factors, intricate land use changes, and small-scale topographical variations that influence erosion rates. Consequently, when validating RUSLE using remote sensing, there is a risk of missing crucial site-specific dynamics essential for accurate assessments, highlighting the necessity of complementary validation methods.

Remote sensing is advantageous in capturing erosion patterns across large areas, but its effectiveness in delivering fine-scale details necessary for robust validation is constrained. Remote sensing data may lack the resolution to consider localized factors, intricate land use shifts, and minor topographical variations that substantially influence erosion rates. Consequently, when validating RUSLE via remote sensing, there is a risk of overlooking crucial

site-specific dynamics essential for accurate assessments. This underscores the necessity of employing complementary validation approaches.

Conversely, local experiments employing the RUSLE model face intricacies stemming from labor-intensive demands. Assembling comprehensive input data for RUSLE, spanning soil characteristics, land use practices, and rainfall patterns, entails substantial fieldwork and data collection endeavors. This calls for skilled labor adept at precise sampling, measurements, and meticulous data recording. Furthermore, calibrating model coefficients to match local conditions necessitates rigorous data analysis and iterative adjustments, further amplifying complexity. The ongoing monitoring and measurement of actual erosion rates for validation require consistent effort involving equipment maintenance, data logging, and the logistical challenges of field campaigns. The labor-intensive nature of local RUSLE experiments underscores the need for dedicated personnel, training, and streamlined coordination to ensure the quality and reliability of the collected data and ensuing model outcomes.

These labor-intensive demands have presented difficulties in conducting field experiments within our research, highlighting the need for efficient coordination and appropriate support to overcome these challenges.

Soil Conservation Initiatives in Sugarcane Areas

As revealed through the referenced studies, the initiatives aimed at soil conservation in sugarcane areas collectively underscore the vital importance of integrating sustainable land management practices into bioenergy production and agricultural expansion in Brazil. These studies offer insightful perspectives on the intricate relationships between land use change, environmental impacts, policy considerations, and the imperative of maintaining ecosystem services.

The intricate interplay between bioenergy production, land-use change (LUC), and sustainability considerations in sugarcane-derived bioenergy is meticulously explored in the review by Cherubin et al. (2021). This comprehensive study, focusing on Brazil's sugarcane-derived bioenergy, underscores the dual challenge of harnessing bioenergy's potential for climate change mitigation while addressing large-scale LUC's environmental and socioeconomic impacts, particularly the expansion of sugarcane crops. By delving into a thorough literature review, the authors meticulously unravel the intricate relationships between LUC, best management practices, and various sustainability components such as soil health, carbon sequestration, greenhouse gas emissions, nutrient cycling, and water quality.

A noteworthy revelation from this review is the potential co-benefits that emerge based on LUC scenarios and management practices. The transition from low-productivity pastures to sugarcane cultivation is highlighted as a promising sustainable pathway that offers advantages in soil health and carbon sequestration. Despite challenges like soil compaction, biodiversity loss, and erosion, integrating best practices such as conservation tillage and rational fertilization is pivotal for sustainable bioenergy production.

The study recognizes the significance of public policies and regulatory frameworks in harmonizing bioenergy production with responsible land use and protection. This is exemplified by Brazil's Forest Code and *RenovaBio* legislations, which serve as important tools for aligning bioenergy production with environmental preservation.

One of the most intriguing insights from Cherubin et al. (2021) pertains to the potential global impact of sugarcane expansion over pasture areas in Latin American, Caribbean, and sub-Saharan African countries. This expansion has the potential to significantly influence global bioenergy supply, underscoring the interconnectedness of local land-use decisions and global sustainability goals.

Complementing the study mentioned above, da Luz et al. (2020) dive into the intricate relationship between sugarcane expansion and soil water dynamics in Brazil's central-south region. Their study highlights the importance of understanding land-use changes' effects on soil hydro-physical properties. While the transition from pasture to sugarcane involves conventional tillage, it intriguingly does not exacerbate soil degradation. Despite slight impairments in soil water and physical conditions in the 100-200 mm soil layer, the study emphasizes the need for sustainable management practices to maintain soil quality and water dynamics, essential for optimal plant growth and broader ecosystem benefits.

Additionally, Picoli & Machado (2021) comprehensively explore Brazil's bioethanol journey, tracing its origins and evolution as a strategy for energy security and reducing greenhouse gas emissions. This paper critically examines the evolution of sugarcane expansion over the years, revealing the complex interplay between bioethanol production and land use change. The study's focus on the indirect consequences of sugarcane expansion, such as encroachment upon pasture areas leading to deforestation, highlights the need for holistic cross-sectoral efforts to ensure biofuel sustainability.

Vera et al. (2020) adopted an integrated approach to investigate the environmental consequences of sugarcane expansion in Sao Paulo state. By aggregating various environmental impacts into an environmental performance index, the study provides a spatially nuanced understanding of the trade-offs associated with sugarcane expansion. Identifying zones with

positive and negative impacts is a foundation for targeted strategies to mitigate adverse effects and enhance favorable outcomes in future sugarcane expansion.

Finally, dos Santos et al. (2020) address the practicality of the Soil and Water Assessment Tool (SWAT) in assessing land use impacts on streamflow and sediment yield. Their study, centered on the Atibaia river basin in São Paulo, highlights the need for well-defined parameter sets to model land use changes' effects on hydrological processes accurately. By pinpointing influential parameters, the research aids in enhancing environmental quality and management practices in the basin.

The collective findings from these studies shed light on the multifaceted challenges and opportunities in soil conservation initiatives within sugarcane areas. It is evident that holistic approaches, incorporating best practices, policy interventions, and innovative modeling techniques, are essential to balance bioenergy production and environmental sustainability. As Brazil's sugarcane industry expands, these studies serve as valuable guides for shaping a future where bioenergy and land conservation coexist harmoniously.

CHAPTER 4. GENERAL REFERENCES

Cherubin, M. R., Carvalho, J. L. N., Cerri, C. E. P., Nogueira, L. A. H., Souza, G. M., & Cantarella, H. (2021). Land use and management effects on sustainable sugarcane-derived bioenergy. In *Land* (Vol. 10, Issue 1, pp. 1–24). MDPI AG. <https://doi.org/10.3390/land10010072>

da Luz, F. B., Carvalho, M. L., de Borba, D. A., Schiebelbein, B. E., de Lima, R. P., & Cherubin, M. R. (2020). Linking soil water changes to soil physical quality in sugarcane expansion areas in Brazil. *Water (Switzerland)*, 12(11), 1–18. <https://doi.org/10.3390/w12113156>

dos Santos, F. M., de Oliveira, R. P., & Di Lollo, J. A. (2020). Effects of land use changes on streamflow and sediment yield in Atibaia River Basin-SP, Brazil. *Water (Switzerland)*, 12(6). <https://doi.org/10.3390/W12061711>

Picoli, M. C. A., & Machado, P. G. (2021). Land use change: the barrier for sugarcane sustainability. *Biofuels, Bioproducts and Biorefining*, 15(6), 1591–1603. <https://doi.org/10.1002/bbb.2270>

Vera, I., Wicke, B., & van der Hilst, F. (2020). Spatial variation in environmental impacts of sugarcane expansion in Brazil. *Land*, 9(10), 1–20. <https://doi.org/10.3390/land9100397>

APPENDIX

Articles

Open Access Article

Soil Erosion Satellite-Based Estimation in Cropland for Soil Conservation

by  Bruna Cristina Gallo ^{1,2} ,  Paulo Sérgio Graziano Magalhães ³ ,  José A. M. Demattê ^{4,*} ,
 Walter Rossi Cervi ^{1,5},  João Luís Nunes Carvalho ²,  Leandro Carneiro Barbosa ² ,
 Henrique Bellinaso ⁴,  Danilo César de Mello ⁶,  Gustavo Vieira Veloso ⁶,  Marcelo Rodrigo Alves ⁷,
 Elpidio Inácio Fernandes-Filho ⁶ ,  Márcio Rocha Francelino ⁶  and
 Carlos Ernesto Gonçalves Reynaud Schaefer ⁶

¹ Interdisciplinary Ph.D. Program in Bioenergy, University of Campinas, Campinas 13083-862, SP, Brazil

² Brazilian Biorenewables National Laboratory (LNBR), Brazilian Center of Energy and Material Research (CNPEM), Campinas 13083-100, SP, Brazil

³ Interdisciplinary Center of Energy Planning, University of Campinas, Campinas 13083-862, SP, Brazil

⁴ Department of Soil Science, Luiz de Queiroz College of Agriculture, University of São Paulo, Piracicaba 13418-900, SP, Brazil

⁵ Wageningen Economic Research, Wageningen University & Research, 6708 PB Wageningen, The Netherlands

⁶ Department of Soil Science, Federal University of Viçosa, Viçosa 36570-900, MG, Brazil

⁷ Department of Environment and Regional Development, University of West São Paulo (UNOESTE), Rod. Raposo Tavares, km 572-Limoeiro, Presidente Prudente 19067-175, SP, Brazil

* Author to whom correspondence should be addressed.

Remote Sens. **2023**, *15*(1), 20; <https://doi.org/10.3390/rs15010020>

Received: 19 October 2022 / Revised: 7 December 2022 / Accepted: 12 December 2022 /

Published: 21 December 2022

MDPI Open Access Information and Policy

All articles published by MDPI are made immediately available worldwide under an open access license. This means:

- everyone has free and unlimited access to the full-text of *all* articles published in MDPI journals;
- everyone is free to re-use the published material if proper accreditation/citation of the original publication is given;
- open access publication is supported by the authors' institutes or research funding agencies by payment of a comparatively low **Article Processing Charge (APC)** for accepted articles.

Permissions

No special permission is required to reuse all or part of article published by MDPI, including figures and tables. For articles published under an open access Creative Common CC BY license, any part of the article may be reused without permission provided that the original article is clearly cited. Reuse of an article does not imply endorsement by the authors or MDPI.

Open Access Article

Multi-Temporal Satellite Images on Topsoil Attribute Quantification and the Relationship with Soil Classes and Geology

by  Bruna C. Gallo ^{1,2} ,  José A. M. Demattê ^{1,2,*} ,  Rodnei Rizzo ¹,  José L. Safanelli ¹ ,
 Wanderson De S. Mendes ¹ ,  Igo F. Lepsch ¹,  Marcus V. Sato ¹,  Danilo J. Romero ¹ and
 Marilusa P. C. Lacerda ³

¹ Department of Soil Science, College of Agriculture Luiz de Queiroz, University of São Paulo, Rua Pádua Dias, 11, Piracicaba, Cx Postal 09, São Paulo, CEP 13416900, Brazil

² Interdisciplinary Program of Bioenergy, University of São Paulo (USP), University of Campinas (UNICAMP) and São Paulo State University (UNESP), Rua Monteiro Lobato, 80, Cidade Universitária, Campinas, SP 13083852, Brazil

³ Faculty of Agronomy and Veterinary Medicine, University of Brasília, Campus Universitário Darcy Ribeiro, ICC Sul, Asa Norte, Cx Postal 4508, Brasília, CEP 70910960, Brazil

* Author to whom correspondence should be addressed.

Remote Sens. **2018**, *10*(10), 1571; <https://doi.org/10.3390/rs10101571>

Received: 27 July 2018 / Revised: 7 September 2018 / Accepted: 26 September 2018 /
 Published: 1 October 2018

(This article belongs to the Special Issue **Selected Papers from the First "Symposia of Remote Sensing Applied to Soil Science"**, as part of the "21st World Congress of Soil Science, 2018")

[Download](#)
[Browse Figures](#)
[Versions Notes](#)

MDPI Open Access Information and Policy

All articles published by MDPI are made immediately available worldwide under an open access license. This means:

- everyone has free and unlimited access to the full-text of *all* articles published in MDPI journals;
- everyone is free to re-use the published material if proper accreditation/citation of the original publication is given;
- open access publication is supported by the authors' institutes or research funding agencies by payment of a comparatively low **Article Processing Charge (APC)** for accepted articles.

Permissions

No special permission is required to reuse all or part of article published by MDPI, including figures and tables. For articles published under an open access Creative Common CC BY license, any part of the article may be reused without permission provided that the original article is clearly cited. Reuse of an article does not imply endorsement by the authors or MDPI.